12-2012

Scopolamine-Induced Dry Eye Model in Female Rats

Ryan Alderson
Western Michigan University

SCOPOLAMINE-INDUCED DRY EYE MODEL IN FEMALE RATS

by

Ryan Alderson

A Thesis
Submitted to the
Faculty of The Graduate College
in partial fulfillment of the
requirements for the
Degree of Master of Science
Department of Biological Sciences
Advisor: Cindy Linn, Ph.D.

Western Michigan University
Kalamazoo, Michigan
December 2012

SCOPOLAMINE-INDUCED DRY EYE MODEL IN FEMALE RATS

Ryan Alderson, M.S.

Western Michigan University, 2012

The objective of this study will be to establish, validate, and characterize a dry eye model in female rats induced by continuous systemic administration of scopolamine via Alzet® osmotic pumps for 28 days. This study will use female rats as a model for dry eye and will be implanted with osmotic pumps that will continuously distribute scopolamine or saline systemically over 28 days. Scopolamine will be used to induce the dry eye condition and saline will be used as a negative control. The clinical signs of dry eye will be evaluated by tear volume measurements with sterilized phenol-red thread (FCI Opthalmics Zone Quick™), corneal staining with 0.2% sodium fluorescein (Novartis Pharmaceutials), and corneal thickness measurements. Ocular coherence tomography (OCT) images of the central cornea will be collected with the Spectralis HRA+OCT (Heidelberg Engineering) to measure thickness and corneal staining will be evaluated using a photographic slit lamp under cobalt blue light (Heidelberg Engineering). Topical medications currently available to treat dry eye will be used in the second phase of the study to validate that the condition is induced and confirm healing. This study will aid in understanding the unique characteristics of dry eye and its limitations to help provide further insight into the development of more effective therapeutic solutions of the condition.

ACKNOWLEDGMENTS

I would like to thank MPI Research for allowing me to take part in this study and to use the research for my Master's thesis project. More specifically, I would like to thank Dr. Thomas Vihtelic and Jeff Jamison, Ph.D. at MPI Research for guiding me through this study and allowing me to work with them on this project.

I would like to thank Cindy Linn, Ph.D. for taking me on as one of her graduate students. Her trust, knowledge, and direction helped me to pull all of the necessary information together and give me the confidence needed to finish this research project.

I would also like to thank John Spitsbergen, Ph.D. and Robert Eversole, Ph.D. for taking the time to sit as members of my Thesis Committee.

I am grateful for the education I have received at Western Michigan University and for the opportunity to complete a scientific research project.

Finally, I would like to thank my family and friends for the love and support they have shown me throughout my life.

Ryan Alderson

TABLE OF CONTENTS

Table of Contents—Continued

Table of Contents—Continued

LIST OF TABLES

List of Tables—Continued

LIST OF FIGURES

SPECIFIC AIMS

The objective of this study will be to establish, validate, and characterize a dry eye model in female rats induced by continuous systemic administration of scopolamine via Alzet® osmotic pumps for 28 days. Dry eye syndrome or keratoconjunctivitis sicca (KCS) is a common ocular disease affecting between 7% and 15% of the female population over the age of 50 in the United States (1). The cornea, conjunctiva, and lacrimal glands comprise the lacrimal functional unit and work together to regulate tear production and character (1). During dry eye, any component of this unit may become inflamed leading to the chronic ocular surface damage that characterizes this condition (1).

Artificial tears offer relief to those suffering from dry eye by improving the symptoms but do not treat the underlying causes that lead to chronic inflammation (2). The key component of pathogenesis in dry eye is inflammation of the ocular surface and, thus, it is the main target for therapy (2). For example, topical administration of cyclosporin A, an immunomodulatory drug, decreases the inflammatory state of the conjunctiva and accelerates the recovery of the conjunctival goblet cells (2).

Comparative animal models of dry eye have been developed to reproduce the pathophysiological effects of this condition (3). This study will use female rats as a model for dry eye and will be implanted with osmotic pumps that will continuously distribute scopolamine or saline systemically over 28 days. Scopolamine will be used to induce the dry eye condition and saline will be used as a negative control. The clinical signs of dry eye will be evaluated by tear volume measurements with sterilized phenol-red thread (FCI Opthalmics Zone Quick™), corneal staining with 0.2% sodium

fluorescein (Novartis Pharmaceutials), and corneal thickness measurements. Ocular coherence tomography (OCT) images of the central cornea will be collected with the Spectralis HRA+OCT (Heidelberg Engineering) to measure thickness and corneal staining will be evaluated using a photographic slit lamp under cobalt blue light (Heidelberg Engineering).

The main objective of this study is to understand the unique characteristics of dry eye and its limitations to help provide further insight into the development of more effective therapeutic solutions of the condition. If we successfully induce dry eye, then the diagnostic methods used to measure ocular dryness will indicate that the condition has been simulated and healing will occur using available topical medications. The three specific aims of this study are:

1. To establish the dry eye condition.
2. Identify symptoms of dry eye using ocular imaging.
3. Confirm that healing can be seen after application of topical medications available to treat dry eye.

The results of this study will provide proven clinical diagnostic procedures to identify dry eye, which topical therapies are most effective in treating the condition, and make a contribution in the field of dry eye study.

INTRODUCTION

Background and Significance

The eyes are a vital sensory organ and provide animals with the sense of sight. The eyes are used to survey the environment and relay sensory information to the brain. Light is one of the most useful signals in the environment and the ability to detect it is, therefore, one of the most useful senses to animals (4). Light from an observed object is focused by the cornea and lens onto the photoreceptive retina at the back of the eye. The focus is maintained on the retina at different distances between the object and the eyes by muscular contractions that change the thickness and degree of curvature of the lens (5). When the light reaches the retina, a signal is sent to the brain via the optic nerve where it is further processed and where visual perception occurs.

Many different cellular structures help provide rigidity to the organ and maintain the overall health of the tissues. The outermost layer of the eye is a tough coat of connective tissue called the sclera, which can be externally seen as the white of the eyes (5). The tissue of the sclera is continuous with the transparent cornea. Light passes through the cornea to enter the anterior chamber of the eye. Light then passes through an opening called the pupil, which is surrounded by a pigmented muscle, known as the iris. After passing through the pupil, light enters the lens, passes through the vitreous chamber, and is focused onto the retina (5). These are the main anatomical structures of the eye and are important for photoreception but they do not function in maintaining the integrity of the tear film and keeping the ocular surface

lubricated. These important functions are the responsibility of the tissues that comprise the lacrimal functional unit.

In order to maintain ocular surface homeostasis, the appropriate release in quantity and composition of tear film components must occur in response to various stimuli. Secretion of tear film components is coordinated and controlled by the lacrimal functional unit. The lacrimal functional unit is composed of the ocular surface tissues, the cornea and conjunctiva, the lacrimal glands (main and accessory), and their interconnecting sensory and autonomic innervation (Cranial Nerves V and VII) (6). Innervation of the lacrimal functional unit occurs from the parasympathetic and sympathetic nerve systems, and sensory fibers from the trigeminal nerve (6).

The cornea protects the delicate intraocular contents with its tough, yet pliable, collagen structure (6). It has the ability to resist injury and provide the essential optics and transparency to focus an image on the retina. The anterior corneal surface becomes slightly flatter in the periphery, giving the overall cornea a naturally rounded shape. If the cornea were perfectly spherical, it would suffer from a considerable spherical irregularity in which the light passing through the peripheral parts of an optical system do not come to the same focal point as the light near the central axis of the system (6). Peripheral corneal flattening reduces the corneal contribution of spherical irregularity to the optical system of the eye. The lens provides additional correction of the residual spherical irregularity of the cornea.

The cornea protrudes slightly beyond the limits of the scleral globe because of the difference in curvature between the relatively steep cornea and the relatively flat globe (6). A shallow sulcus is formed at the intersection of the corneal and scleral surfaces, which roughly defines a region called the limbus. The histologic limbus is the full-thickness annular boundary that separates the optically transparent corneal stroma

from the opaque sclera (6).

The corneal epithelium is the anterior-most cell layer of the cornea. It is typically several cell layers thick, consisting of the apical squamous cell layer, the multilayered, polygonal-shaped wing cells beneath the apical layer, and the posterior-most layer of basal cells (6). The wing cell layer is two or three cells thick in the central cornea, but tends to be four to five cells thick in the periphery. The two major properties of the corneal epithelium needed for normal vision are to form a smooth refractive surface via its interaction with the tear film and to form a protective tight junctional barrier that prevents decreases in net fluid transport out from the stroma and prevents corneal penetration by pathogens (7). To provide the epithelial barrier function, epithelial cells are specialized to form tight adherences between one another and to the basal lamellae. The cells from the basal layer migrate into the suprabasal layers and undergo differentiation. The superficial cells possess tight junctions, zonulae occludens, which serve as a semipermeable, highly resistive membrane (7). As the superficial differentiated cells are lost, they are replaced by the underlying proliferating basal cell layer. Following their emergence, the newly formed cells migrate first from the basal layer into the upper differentiating wing layers and then into the superficial layers. It is of paramount importance that the differentiating cells are able to re-establish the tight junctional physical barrier that protects the cornea interior from noxious agents, e.g., microorganism infections, as the epithelial cell layers are interconnected via desmosomes and communicate with one another via gap junctions, especially in the wing cell layer. Therefore, through the processes of mitosis, migration, and shedding, the cornea epithelium is well maintained (7). The Bowman's membrane lies just beneath the epithelium. Because this layer is very tough and difficult to penetrate, it protects the cornea from injury. It is located between the

superficial epithelium and the stroma in the cornea. It is composed of strong collagen fibers and helps the cornea maintain its shape. In total, the epithelium is approximately 50 micrometers (μm) thick in the central human cornea (7).

The epithelium is in a constant state of turnover, with exfoliating apical cells being replaced by the underlying wing cells (6). During normal exfoliation, desquamating cells are released only after the replacement cell has established new tight junctions with neighboring cells and the new apical membrane is capable of maintaining continuity of the tear film (6). Studies of induced exfoliation of a monolayer of epithelial cells with a biologic detergent indicate recovery of the paracellular barriers and transepithelial electric resistance in approximately 1 hour (hr) (6). The epithelium completely turns over in approximately seven days (6). Once injured, a high degree of motility ensures coverage of a discarded area by adjacent basal cells, followed by replacement of the normal complement of cell layers. Basal cells are the only epithelial cells capable of mitosis; however, many epithelial cells originate as the progeny of limbal stem cells and migrate to supplement or replace cells lost through normal desquamation or injury (6). Using immunohistochemical (IHC) staining for antibodies to keratins, Wiley, *et al.* (2006), found regional heterogeneity indicating that the superior corneal periphery and limbus have the greatest numbers of stem cells producing replacement epithelial cells (6). Limbal stem cell deficiency may result in conjunctival epithelium invasion of the cornea, leading to vascularization, the appearance of goblet cells, and an irregular or unstable epithelium that reduces visual acuity and may produce pain or discomfort (6).

The corneal epithelium is known to chemically interact with keratocyte cells of the stroma. These interactions appear to be dominated by cytokines such as interleukin-1 (IL-1) and soluble Fas ligand that are released by injured epithelial cells

(6). It is presumed that IL-1 is a master regulator for corneal wound healing given its effect on keratocyte apoptosis and the modulation of matrix metalloproteinase and growth factors such as keratinocyte growth factor (KGF) and hepatocyte growth factor (HGF) (6). The Fas ligand system is known to influence the immune state of the cornea. In addition to the epithelial-to-keratocyte communication, keratocytes influence the state of the epithelium via HGF and KGF, which affect cell turnover, motility, and proliferation (6).

In dry eye, climate is a potential causative agent and people living in dry, arid environments (i.e. retirees in Arizona) experience symptoms associated with the condition. While the exact cause of these symptoms remains unclear, ocular dryness due to increased tear evaporation may be due to low humidity, high room temperature and air velocity, decreased blink rate, or indoor pollution or poor air quality (8). Due to the fact that the epithelium is the outermost layer of the cornea, this cell layer is directly exposed to the external environment and will be a particular area of interest during this study because injury to these cells will be indicative of dryness to the ocular surface. Corneal staining will indicate whether injury has occurred and graded using the scoring system suggested by Viau, *et.al.* (2008) (1). Corneal thickness will be another area of interest because the interactions the corneal epithelium has with keratocyte cells, growth factors, the Fas ligand system, and cytokines will indicate that an inflammatory response due to injury is present and wound healing has occurred.

The conjunctiva is a thin, semitransparent mucous membrane that covers the posterior surface of the eyelids and is then reflected onto the eyeball, where it extends to the edge of the cornea (9). The conjunctiva takes its name from the fact that it conjoins the eyelids with the eyeball (9). This junction is indirect, with the conjunctiva forming a fornix on three sides of the globe and an extendible plica on the fourth side

(9). The fornixes and plica of the conjunctiva are loose arching folds connecting the conjunctival membrane lining the inside of the eyelid with the conjunctival membrane covering the eyeball. This arrangement allows the globe and eyelids to move independently of each other (9).

The cellular structure and organization of the conjunctiva is nonkeratinizing squamous epithelium containing mucin-secreting goblet cells (9). This epithelium overlies a loose connective tissue, the substantia propria, which is highly vascularized, contains afferent and efferent sensory innervation and is rich with lymphoid tissue. The conjunctiva functions to enable independent motion of the globe and eyelids but it also protects the cornea and the interior of the eye from the external environment by secreting mucins, antibacterial proteins, electrolytes, and water to form the inner mucous layer of the tear film and possibly a portion a of the aqueous layer. Without these normal conjunctival secretions, a variety of mucous-deficiency diseases develops and can lead to extensive damage to the cornea and sight-threatening conditions (9).

The conjunctiva may be divided into three major subdivisions: the tarsal, or palpebral, lining the eyelids, the forniceal, lining the upper and lower fornices, and the bulbar, overlaying the sclera on the anterior portion of the globe (9). The tarsal conjunctiva lies in a shallow groove called the subtarsal groove (9). This groove runs parallel to the eyelid margin for most of the length of the tarsal conjunctiva. The groove marks the area of transition from the nonkeratinized, stratified squamous epithelium of the eyelid margin to the cuboidal epithelium of the tarsal conjunctiva. The groove provides an ideal anatomical trap for small foreign objects before they can reach the cornea and bulbar conjunctiva. The objects trapped in the subtarsal groove are covered with a thick coating of mucus and are moved medially by the blink to be carried out on, and trapped by, the hairs of the caruncle. There are multiple smaller

ridges and grooves between the eyelid margin and the tarsal groove that contain a series of small saccular mucus glands. Each of these glands has a tubular lumen that opens onto the conjunctival surface. These glands are formed by an invagination of the conjunctival epithelium and are lined with mucus-secreting epithelial cells (9).

The bulbar conjunctiva is smoother than the palpebral conjunctiva and its surface features are less consistent. There are often four to six low broad papillae about the corneoscleral limbus that range in size. The palisades of Vogt are structures around the limbus that radiate outward from the cornea. One of their functions is to trap small foreign objects that were on the cornea and were subsequently dislocated by blinking. The palisades are often outlined by a fine brown line that radiates from the cornea. This is caused by the production of pigment from an increase in the local melanocyte population, which makes these structures easy to identify (9).

The basal conjunctival epithelial cells are attached by desmosomes to a basement membrane. The tarsal conjunctiva is firmly attached to the tarsi. Meibomian glands are visible in both the upper and lower eyelids as yellow streaks running perpendicular to the eyelid margin. From the fornices, the conjunctiva sweeps posteriorly to attach to and cover the eyeball. Medially it variably covers the globe posterior to the limbus. The conjunctiva forms four fornices where it is reflected from the eyelids to the globe (9).

In addition to the epithelial cells, goblet cells are the second cell type found in the conjunctival epithelium and are the main source of mucus secretion. Found singly or in clusters, goblet cells are dispersed among the stratified squamous cells of the conjunctival epithelium. Goblet cells contain secretory granules in the apical portion of the cell that contain the mucins and other glycoproteins that are secreted onto the mucus layer of the tear film. MUC5AC, the large gel-forming mucin that is the major

mucin present at the ocular surface, has been identified to be associated with the goblet cells, but other mucins, such as MUC2 and MUC7, may also be associated (9).

The main lacrimal gland is located in the superotemporal orbit in a shallow lacrimal fossa of the frontal bone and it is surrounded by fibrous tissue that is attached superiorly to the frontal bone periosteum (10). It is incompletely divided into a larger orbital lobe, which comprises 60% to 70% of its total mass, and a smaller palpebral lobe below. Blood vessels, nerves, and the lacrimal ducts connect the two lobes (10).

The lacrimal gland is divided into numerous lobules, separated by interlobular fibrovascular connective tissue. Each lobule is structurally composed of the acinar unit and the ductal system (9). Two to six secretory ducts from the orbital lobe of the lacrimal gland pass through the palpebral lobe or along its fibrous capsule, joining with ducts from the palpebral lobe to form six to twelve tubules that empty into the superolateral conjunctival fornix above the tarsus (10). The ducts, lined by pseudostratified, nonkeratinizing squamous epithelium, form a branching pattern within the lacrimal gland. Secretion from the acinar units first drains into the smaller intralobular ducts, proceeds through the larger interlobular ducts, and eventually passes into the main excretory ducts before draining into the superolateral conjunctival fornix (9). The surface of the ductal lumina contains microvilli, similar to the acinar secretory cells. The epithelial walls of the larger ducts contain three to four layers of columnar or cuboidal cells, compared with a single layer in the smaller intralobular ducts (9).

Each acinar unit, or secretory unit, of the lacrimal gland is composed of an inner layer of columnar or pyramid-shaped secretory cells around a central lumen, and a surrounding basal layer of myoepithelial cells (10). The nucleus is located at the base of the acinar secretory cell, and numerous membrane-bound zymogenic secretory

granules are present in the apical cytoplasm (10). The number and size of granules, which contain predominantly serous proteins for secretion, vary from cell to cell. Typically, larger granules are located in the peripheral lobules (10). The zymogenic secretory granules fuse with the apical cell membrane and release their granular contents into the acinar lumen through exocytosis (10). Myoepithelial cells are spindle- or basket-shaped cells, composed of cytoplasmic myofilaments, located between the base of the secretory cell and the basement membrane of the acinar unit (10). Contraction of the myoepithelial cells helps drive secretions into the drainage tubules and ducts (10).

Accessory lacrimal glands are located in the conjunctival fornices and along the superior tarsal border (10). There are approximately twenty to forty accessory glands in the superior conjunctival fornix (10). There is approximately half the number of glands present in the lower eyelid as in the upper eyelid (10). Slightly larger accessory glands are located along the superior tarsal border in the upper eyelid and in the lower eyelid (10). The accessory lacrimal gland lobules empty onto the conjunctival surface through small branching ducts that drain into a single excretory duct that is lined by one or two layers of cells (10).

The accessory lacrimal glands are innervated like the main lacrimal gland (10). Parasympathetic, sympathetic, and sensory nerves have been identified in accessory lacrimal glands of human tissue (10). The presence of nerves suggests that secretion from accessory lacrimal glands is regulated by the nervous system, which suggests that the accessory lacrimal glands can also contribute to stimulated tear secretion (10).

The lacrimal gland secretes water, electrolytes, and proteins in response to neural and hormonal stimulation and is the major contributor to the aqueous portion of the tear film with additional contributions from the accessory lacrimal glands, the

cornea, and the conjunctiva (10). Parasympathetic nerves, containing acetylcholine (ACh) and vasoactive intestinal peptide (VIP), and sympathetic nerves containing norepinephrine (NE), provide strong stimuli of lacrimal gland secretion (10). In addition, many hormones from the hypothalamic-pituitary-gonadal axis have significant influences on the lacrimal gland, including stimulating secretion of secretory immunoglobulin A (SIgA) (10). Sensory nerves are the least prevalent and release substance P and calcitonin gene-related peptide. In the lacrimal gland, each of these agonists binds to specific receptors on the acinar cells and initiates a different cascade of cell signaling transduction pathways (10).

Tear film secretion from the lacrimal functional unit is reflexive (12). The sensory nerves of the highly innervated cornea and conjunctiva form the afferent limb of a simple reflex arc that conducts stimuli from the external environment back to the central nervous system (12). The efferent limb of the reflex arc is composed of the sympathetic and parasympathetic nerves that innervate the ocular surface epithelia and tear-producing glands (12). These nerves are responsible for stimulating the conjunctival epithelial goblet cells, lacrimal glands, and meibomian glands to secrete their respective components (mucus, aqueous, and lipid, respectively) onto the ocular surface to provide protection from the original stimulus (12).

The tear film is responsible for providing a smooth refractive surface for clear vision, maintaining the health of corneal and conjunctival epithelia, and acting as the first line of defense against microbial infections (12). Tear film composition is dynamic and in a constant state of flux, responding to environmental conditions in order to maintain ocular surface homeostasis. Traditionally, the tear film was described as being composed of three separate and distinct layers: mucin, aqueous, and lipid (12). However, new studies suggest that mixing between the mucin and aqueous

layer occurs which creates a gradient of decreasing mucin concentration into the aqueous layer (12). This aqueous-mucin layer forms a complex, hydrated gel, which is then covered by the lipid layer, which has its own highly ordered structure (12).

The majority of ocular mucins are secreted by the conjunctival goblet cells (12). Ocular mucus is composed of mucin, immunoglobulins, urea, salts, glucose, leukocytes, cellular debris, and enzymes (12). Mucins are high molecular weight glycoproteins that are heavily glycosylated where 50% to 80% of their mass can be attributed to their carbohydrate side chains (12). Tandem repeats of amino acids rich in serine and threonine found in their protein backbone serve as sites for O-type glycosylation (12). Heavy glycosylation contributes an overall negative charge to the glycoprotein, making the mucins highly hydrophilic and able to mix with the aqueous layer and maintain water on the surface of the eye (12).

Mucins are classified as either membrane-associated or secretory. Secretory mucins are further divided into two groups: large gel-forming mucins or small soluble mucins (12). Secretory mucins act as a "cleaning crew," moving through the tear fluid and collecting debris that can then be removed via the nasolacrimal duct during blinking (12).

Large membrane-associated mucins form the glycocalyx, a dense barrier to inhibit pathogen infiltration, at the epithelial cell–tear film border (11). Secreted mucins move easily over the mucins composing the glycocalyx because of the repulsive forces between them, which result from their anionic character (12). The membrane-associated mucins contain a hydrophobic transmembrane domain that anchors the mucin on the apical surface of the epithelial cells, a short cytoplasmic tail that extends into the cytoplasm, and an extracellular domain that reaches into the tear film (12). The extracellular, highly glycosylated tandem repeat domains, also called

ectodomains, function to prevent adhesion via cell–cell and cell–matrix interactions (12). This property provides a lubricating surface that allows eyelid epithelia to glide over the corneal and conjunctival epithelia without adherence (12). The cytoplasmic tail of the membrane-associated mucin is thought to affect epithelial activity by interacting with cytoplasmic proteins and facilitating signal transduction (12). The short cytoplasmic domains are also reported to be associated with the actin cytoskeleton, which helps support the microplicae structure (12).

Soluble forms of the membrane-associated mucins have also been identified in the tear film, although the exact mechanisms for this occurrence are still unknown (12). Possible mechanisms include: cleavage and release of the extracellular domain into the tear film in a process termed ectodomain shedding, posttranslational processing of the mucin into two subunits where one subunit remains anchored in the plasma membrane and the other soluble subunit is packaged in secretory granules and released into the tear film, or mucin shedding from the cell surface over time leaves the oldest cells without microplicae and membrane associated mucins, which results in the adherence of the old cells to the mucus of the tear film and their removal via the nasolacrimal duct (12).

The middle aqueous layer of the tear film consists of water, electrolytes, proteins, peptide growth factors, immunoglobulins, cytokines, vitamins, antimicrobials, and hormones secreted by the lacrimal glands (12).

Electrolytes present in the tear film include sodium, potassium, magnesium, calcium, chloride, bicarbonate, and phosphate ions. These electrolytes are responsible for the osmolarity of tears, acting as a buffer to maintain a constant pH and contribute to maintaining epithelial integrity of the ocular surface. An increase in osmolarity of the aqueous layer is a global feature of dry eye syndrome and damages the ocular

surface directly and indirectly by triggering inflammation (12).

More than sixty proteins have been identified in human tears including albumin, immunoglobulins, metal-carrying proteins, histamine, plasminogen activator, prostaglandins, proteases, and antimicrobials (12). Considering that the thin, nonkeratinzed epithelium and abundant blood supply of the conjunctiva make the conjunctiva an ideal entrance for infectious agents, it is imperative that the ocular surface has a strong defense system to protect against invading microorganisms (12). The primary defense system of the ocular surface is composed of the nonspecific immunity presented by lysozyme, lactoferrin, β-lysin, defensins, and group II phospholipase A and the specific immunity of antibodies (12). Immunoglobulins are constitutively produced and transported to the tear film from the conjunctiva. Thus, reflex tearing reduces the concentration of immunoglobulins and a reduction in tear flow increases their concentration (12). In aqueous-deficient dry eye syndrome, the concentration of lysozyme, lactoferrin, lipocalin, and SIgA are reduced, compromising the integrity of the defense system, which may make the ocular surface more susceptible to infection, in addition to the symptoms of dry eye (12).

The anterior layer of the tear film is composed of meibomian oil secreted by the meibomian glands and is the major barrier to evaporation from the ocular surface (12). The lipid layer is also responsible for providing stability to the tear film through interaction with the aqueous-mucin phase, providing a smooth optical surface for the cornea, and acting as a barrier against foreign particles (12). Oil secretion is a continuous process, occurring twenty-four hours per day during waking and sleeping hours, and is aided by blink action. The rate of secretion is controlled by neural, hormonal, and vascular influences (12). A normal tear film lipid layer is able to reduce evaporation by approximately 90% to 95% (12). The rate of evaporation is affected

by the thickness of the lipid layer, and it has been proposed that a decrease in thickness may cause evaporative dry eye (12). Mild to moderate dry eye states exhibit a lack of confluence in the tear film lipid layer (12).

The conjunctiva, lacrimal functional unit, and tear film all work together to maintain the integrity of the ocular surface and provide a moisture-rich environment. If any of these components is compromised, the eye may become susceptible to infection and disease. In the case of dry eye, evaporation of the tear film may be caused be environmental factors such as a dry, arid climate or dysfunction of the lacrimal unit. Evaporation may also be caused by the lack of lipids protecting the aqueous layer of the tear film due to dysfunction of the meibomian gland. This dryness causes discomfort and pain therefore decreasing quality of life. Understanding how these cells and tissues function together is crucial to discovering the cause of dry eye but in order to determine if a patient has dry eye, the proper diagnostic measures must be made and the efficacy of available drugs must also be evaluated. The dry eye model used in this study intends to provide this information.

Classification of Dry Eye Animal Models

Lacrimal Inflammation

A number of animal models of dry eye have been developed including rabbit, mouse, rat, canine, feline, and primate. Several animal models studying lacrimal inflammation have been developed, with particular attention to the early activation and infiltration of autoreactive lymphocytes (3). The nonobese diabetic (NOD) mouse model shows a lymphocytic infiltration of predominantly $CD4^+$ Th1 cells in the lacrimal gland (13). Male NOD mice show significant inflammatory lesions of the lacrimal gland from the age of eight weeks, whereas female NOD mice do not show

any changes until thirty weeks of age. Although significant attention has focused on lacrimal lesions in NOD mice, the only published study demonstrating altered tear secretion in these mice reported a reduction by 33 – 36% compared with wild-type animals; a reduction rate that is less profound than the decreased lacrimal function in patients exhibiting lacrimal inflammation (14). The consequences of the reduced tear production of the ocular surface epithelium of these mice have never been definitively demonstrated and suggest this model is better fitted for studying secondary but not primary lacrimal inflammation (13).

The MRL/MpJ-*fas*$^{+}$/*fas*$^{+}$ (MRL/+) and MRL/MpJ-*fas*^{lpr}/*fas*^{lpr} (MRL/lpr) mouse models of lacrimal inflammatory syndrome exhibit lacrimal gland infiltrates characterized by a predominance of $CD4^{+}$ T cells (15). In contrast to the NOD model, the extent of the lacrimal gland inflammation is significantly greater in lacrimal glands of female MRL/+ and MRL/lpr mice than is observed in males, resembling the difference observed in human lacrimal inflammatory syndrome (16). In the MRL/lpr mouse, the lacrimal gland inflammation has an earlier onset (1 month of age) and a greater severity at same ages as in the MRL/+ mice (onset at 3 months), indicating that the *lpr (*lymphoproliferation) mutation accelerates, rather than causes the disease. The defective lymphocyte apoptosis (thought to regulate T cells reactivity naturally) in MRL/lpr mice due to an *lpr* mutation in a single autosomal recessive gene controlling the Fas antigen occurs systemically and outside the lacrimal gland, and therefore is not itself due to the micro-environment of the lacrimal gland in this mouse model. According to Toda, *et. al.* (1999), the *lpr* gene itself does not cause severe immunopathologic lesions in the lacrimal tissue, since male C3H/lpr and *gld* (generalized lymphoproliferative disease) mice show almost no lymphocyte accumulation in the lacrimal gland (16). These findings seem to support the

hypothesis that Fas antigen and Fas ligand are not critical gender- and strain-independent determinants of autoimmunity in lacrimal tissue (17). The immunopathology of this model is unique, in that the predominance of IL-4 and B7-2 within the lacrimal gland lesions of MRL/lpr mice suggests a largely Th2-type response, distinct from that in the NOD model (18). Overall, these data suggest the existence of potentially divergent immunopathogenic mechanisms to lacrimal autoimmunity in the mouse (3).

Autoimmune phenomena in F1 hybrids of New Zealand Black and New Zealand White (NZB/NZW F1) mice are comparable to MRL/lpr mice and are similarly more severe in females than in males, but lesions in the lacrimal glands of the F1 mice become evident after only 4 months instead of 1 month (18). The effect of lacrimal inflammation on the ocular surface of these mice is poorly described. In fact, Gilbard, *et. al.* (1987), demonstrated the lack of corneal epithelium abnormalities in NZB/NZW F1 mice along with a normal tear film osmolarity, despite the lacrimal gland infiltration, emphasizing the important point that lacrimal and ocular surface disease do not necessarily correlate (19).

There are several other other murine models that are also associated with a predominant $CD4^+$ T lymphocyte infiltration of the lacrimal gland (3). The TGF- β1 knockout mouse, for example, has shown significant inflammatory cell infiltrates in the lacrimal gland between the ages of 2 and 4 weeks, whereas the globe itself exhibits a normal structure and phenotype upon histologic examination (20). Unfortunately, shortly after weaning, the mice begin to show the symptoms of a wasting syndrome and die between three and four weeks. Providing liquid diet supplements at the time of weaning prolongs survival of TGF-ß1 knockout mouse almost twice as long as providing standard hard diet, thus enabling longer observation of these mice (21). The

shortened life of the TGF- β1 knockout mouse generally complicates their use as a model, particularly for studies involving testing of therapeutics (3).

Mice homozygous for an autosomal recessive mutation, alymphoplasia (*aly*), which causes a systemic absence of lymph nodes and Peyer's patches, have also been demonstrated to have infiltration of $CD4^+$ T cells into their lacrimal and salivary glands, lung, liver, kidney, and pancreas, potentially serving as a model of lacrimal inflammatory syndrome (22). In particular, lymphocytic infiltrates can be detected in the lacrimal gland from the age of 14 weeks in both males and females. Several factors complicate the use of these mice for study of ocular surface disease. First, no definitive data have been produced relating the lacrimal gland infiltration to altered tear secretion in these mice. Second, the absence of lymph nodes, together with a variety of other serious immune defects, including depressed baseline immunoglobulin production and isotype switching, defective T cell function, and faulty homing responses, all confound the study of the effect of lacrimal insufficiency on the eye, as each of these factors alone or in combination may affect the cornea and ocular surface (3).

The IQI/Jic has recently been established as a new mouse model for primary lacrimal inflammatory syndrome. Unlike the NOD model, in the IQI/Jic mouse the lymphocytic infiltration is well restricted to salivary and lacrimal glands (3). Konno, *et. al.* (2003), have suggested that in this model, the early phase of adenitis (lacrimal inflammation) is mediated by dendritic cells that promote induction of Th1-type immunity, which may also be potentiated by lacrimal epithelial cells that also function as secondary antigen-presenting cells (APCs) (23). The general phenotype of this mouse model of lacrimal inflammatory syndrome makes it quite attractive for the study of the early phases of the disease, even if the development of complete dacryoadenitis

(lacrimal inflammation) at an advanced age (9 months) makes it economically unappealing. Another model for inducing salivary and lacrimal gland specific lymphocytic infiltration, but at a more rapid pace, has been developed by injecting mononuclear cells isolated from the inflamed submandibular salivary tissues of MRL/lpr mice intraperitoneally into *Scid* mice (3). At 8 weeks after the injection, these *Scid* mice exhibit inflammatory lesions in the salivary and lacrimal glands, but not in other organs, confirming the tissue-specificity of disease in these animals. Of interest, the injection of lymphocytes from the spleen of the MRL/lpr mice have not produced any inflammatory lesions in *Scid* mice (24).

Human lacrimal inflammatory syndrome is characterized by the presence of serum autoantibodies to the ribonucleoprotein particles SS-A (anti-SS-A/Ro, 52 kDa; anti-SS-A/Ro, 60 kDa) and SS-B (anti-SS-B/La) (25), and, as recently demonstrated, anti-120-kDa α-fodrin (26), and anti-M3 and -M1 muscarinic acetylcholine receptors (27). Autoantibodies are also present in the serum of NOD and MRL/lpr mice, but with a different pattern of expression than what is observed in humans (3). The role of autoantibodies in NOD mouse has been postulated based on the observation that NOD $Ig\mu^{null}$ mice (lacking B lymphocytes) maintain normal secretory function, even in the presence of focal infiltrates in the salivary gland, suggesting that humoral immunity plays a critical role in the pathogenesis of autoimmunity in these animals (28). Furthermore, the infusion of anti-M3 muscarinic receptor antibodies into NOD-*Scid* mice produces a decreased salivary response (29). To date, there have been no published data about the influence of anti-M3 muscarinic receptor antibodies on tear production (3).

Finally, NFS/sld mice thymectomized at 3 days of age (3d-Tx NFS/sld) have also been used as a model of primary lacrimal inflammatory syndrome to identify the

autoantigen 120-kDa α-fodrin (26). In particular, this autoantigen, purified from the salivary glands of 3d-Tx NFS/sld mice, postulated as the presenting antigen in salivary gland disease in lacrimal inflammation, has been demonstrated to be the product of caspase 3 cleavage of the 240-kDa α-fodrin, rendering this model ideal for study of the mechanism of apoptosis in lacrimal inflammatory syndrome. However, the profound effect of the thymectomy on the endocrine-immune system limits the use of this model for long-term prospective studies (3).

Rabbits have a much larger ocular surface compared to mice which makes performing studies on these animals much easier. Zhu, *et. al.* (2003), induced an autoimmune disease in rabbits resembling lacrimal inflammatory syndrome by injecting into the lacrimal gland autologous peripheral blood lymphocytes proliferated in culture with epithelial cells obtained from the contralateral excised gland (30). The histopathologic picture of the lacrimal glands so treated was similar to the findings in patients with lacrimal inflammartory syndrome, with predominantly $CD4^+$ T cell infiltrates (30). A continuous decrease in tear production and stability and an increase in rose bengal staining of the ocular surface, were recorded in eyes injected with activated lymphocytes and in the contralateral lacrimal gland–excised eyes by 2 weeks, indicating a generalized autoimmune phenomenon (30). An important lingering point to verify in this model is whether the acinar cell preparation (the putative APCs of this model) is completely devoid of any professional bone marrow–derived APCs that can stimulate the T cells (3).

Experimental immune dacryoadenitis has been produced in Lewis rats by sensitization with a single intradermal administration of an extract of lacrimal gland in complete Freund's adjuvant (CFA) and simultaneous intravenous injection of killed *Bordetella pertussis* (31). No data have been published about the effect of this

procedure on the ocular surface (3).

Mechanical Control of Lacrimal Secretion

In dogs, cats, rabbits, and mice the removal of the main lacrimal gland produces a decrease in basal tear production as measured by the Schirmer test, but it does not cause significant changes in ocular surface signs, even after a long follow-up (3). This may be due to accessory lacrimal glands that could provide an adequate compensatory tear supply. In rabbits, closing the lacrimal gland excretory duct and surgically removing the nictitating membrane and harderian gland can cause an increase in tear osmolarity at postoperative day 1 accompanied with significant decrease in conjunctival goblet cell density by 8 weeks (3).

Monkeys have one main lacrimal gland with an anatomic structure similar to that in humans. The removal of the lacrimal gland has been demonstrated to decrease tear secretion, but without producing any reproducible ocular surface damage (32). As in other species, it is thought that compensatory tear production by the accessory lacrimal glands alone may be sufficient enough to maintain a stable tear film (3).

Endocrine Control of Lacrimal Secretion

Spontaneous development of dry eye due to specific endocrine imbalance has not been shown in any animal models to date. Nevertheless, orchiectomy and ovariectomy in rabbits, rats, mice, guinea pigs, and hamsters, and hypophysectomy in rats, have been used as models to study the influence of hormones on the structure and function of the lacrimal and meibomian glands (3). These procedures are not meant as an exact mimic of dry eye, but to decipher important pathogenic aspects of tear film regulation (3). Hormones have both direct and indirect effects on exocrine tissues due

to their capacity to regulate immunity as well as the gene expression of many secreted molecules. For example, Sullivan, et. al. (2002), have demonstrated that androgens regulate the function of lacrimal glands and the quantity, quality, and metabolism of the lipid layer of the tear film produced by the meibomian glands (33). This may be an indication why women in the U.S. over the age of 50 display increased signs of dry eye because they have gone through menopause which causes a change in estrogen levels. Genetically modified mice are expected to aid in the study of the influence of a specific hormone(s) on the tear film homeostasis (3).

Neuronal Control of Lacrimal Secretion

The ocular surface (cornea, conjunctiva, and accessory lacrimal glands), meibomian glands, and main lacrimal gland, are interconnected by neural reflex loops that maintain an integrated "functional unit" (34). The only dry eye animal model described in the literature that supposedly mimics a blockade of the neural reflex loops involved in maintaining the normal tear physiology has been created by administrating the anticholinergic agent atropine in New Zealand albino rabbits (3). The antimuscarinic effect of topical 1 % atropine sulfate has been shown to reduce lacrimal secretion significantly within 2 days and to induce corneal epithelial defects by 3 days (35). Intramuscular doses of atropine are not recommended for use, because they produce toxic systemic side effects and fail to induce corneal damage (3).

The MLR/lpr mouse model has been used to test the hypothesis that a reduction of the quantity of parasympathetic fibers, or an alteration in the neurotransmitters in the healthy tissue of the lacrimal gland, is responsible for tear decrease in patients with lacrimal inflammatory syndrome (3). Zoukhri, *et. al.* (1998), have shown, however, that in the MRL/lpr model, parasympathetic, sympathetic, and

sensory innervations of the lacrimal gland are not altered and the Ca^{2+} signaling portion of cholinergic nerve transmission is indeed up regulated with the onset of lymphocytic infiltration in these mice, suggesting that inadequate innervation of exocrine tissue alone cannot explain the partial deficit in lacrimal secretion (36).

Evaporative Dry Eye

The ocular surface is constantly exposed to multiple environmental factors which may lead to evaporation, including low humidity, high room temperature and air velocity, decreased blink rate, or indoor pollution or poor air quality (10). The lipids produced by the meibomian glands and spread onto the aqueous phase by the shear forces produced by each blink, protect the tear film from excessive evaporation (3). Short-term models for hyperevaporative dry eye have been created by preventing rabbits from blinking through placement of lid specula or sutures (3). After two hours of desiccation induced by lid specula, dry spots appear on the rabbit corneal epithelial surface and stain with methylene blue (37). Because of the acuteness of the induced dry eye and the use of anesthetics (which themselves can decrease tear secretion), these models are not optimal for studying KCS pathogenesis, which is a chronic event. However, in these rabbits, corneal epitheliopathy develops within a few hours, and hence such rabbits can be used to evaluate the effect of artificial tears or other therapies aimed at delaying the evaporative loss of the tear film (3).

Histopathologic and clinical studies indicate that meibomian gland duct orifice closure is a characteristic feature of meibomitis-related dry eye (3). The first objective evidence in support of this hypothesis was provided by Gilbard, *et. al.* (1989) who used a rabbit model in which the meibomian gland orifices were individually closed by cauterization (38). They demonstrated not only a significant decrease in conjunctival

goblet cell density and corneal epithelial glycogen levels by twelve weeks, but also the presence of inflammatory cells within the bulbar conjunctiva after twenty weeks (38). Although this model is an interesting one for studying the effect of meibomian gland dysfunction on the ocular surface, this is best done in a controlled environment in which temperature, humidity, and airflow are constantly monitored and controlled (3). This would more closely reflect the clinical setting, where it has been demonstrated that the tear film evaporation rate from the ocular surface is temperature-, humidity-, and airflow-dependent (39). Recently, several novel mouse models of meibomian gland dysfunction have been created. These models provide new insights into the pathophysiologic mechanisms of hyperevaporative dry eye and identify potential novel gene therapy targets (3).

Combined Lacrimal Insufficiency and Evaporative Dry Eye Models

Dursun, *et. al.* (2002), have presented a mouse model of KCS in which transdermal scopolamine application and exposure to a continuous airflow are used to induce dry eye in female mice (40). The function of scopolamine is to induce a pharmacologic blockade of cholinergic (muscarinic) receptors in the lacrimal gland and therefore to decrease aqueous production, whereas the airflow is to mimic environmental stressing conditions (with resultant increased evaporation) (40). Alterations to aqueous tear production and volume, tear clearance, corneal barrier function, conjunctival morphology and goblet cells density, resemble those of human KCS. However, the tear production has been shown to be reduced only in the group of mice treated with scopolamine, whereas the airflow does not appear to influence the tear film and ocular surface signs (3). Although there are significant benefits to studying sicca-related ocular surface disease in mice that do not have concomitant

systemic immune dysfunction, this model has yet to be optimized, as it does not adequately control important environmental factors such as temperature and humidity—important factors that can have profound effects on the exposed ocular surface (3). Moreover, the airflow generated by an air fan placed six inches in front of the mice's cage for ten hours a day for twelve consecutive days may be a source of stress for mice and therefore influence the data on the tear film homeostasis. This may be a model that best represents the neural inhibition of tear secretion through pharmacologic inhibition of cholinergic pathways more than a "pure" hyperevaporative dry eye model (3).

Spontaneous KCS

In 1979, Quimby first recognized the similarities between the dogs with severe KCS, xerostomia, vaginal dryness, and multiple serum antibodies and lacrimal inflammatory syndrome in humans (3). This likeness has been confirmed lately by a study of lacrimal glands and conjunctiva in KCS dogs by TUNEL (Terminal deoxynucleotidyl transferase dUTP nick end labeling) assay, revealing a decrease in apoptosis in the lymphocytes infiltrating the lacrimal gland and an increase in apoptosis in lacrimal acinar and conjunctival epithelial cells (41). The spontaneous canine dry eye model has been widely used to develop therapeutic interventions for both veterinary and clinical populations, as exemplified by trials on topical application of cyclosporin A (42). The incidence of KCS in the general canine population is unknown, although in one study of 460 dogs, the prevalence was estimated at 35%, with particular predisposition among aged dogs of either sex (42). The breed with the highest relative prevalence of KCS is the American cocker spaniel (20.6%), whereas the commonly used laboratory dogs such as mixed-breed and beagle dogs have lower

prevalence rates of 11.5% and 1.2%, respectively (42). Even if there are multiple causes of canine KCS (i.e. distemper virus, drug-induced), most are of undetermined origin and may be immune mediated. Spontaneous KCS in dogs provides a very useful model for dry eye studies: the large size of the dog's globe compared with that of the mouse provides benefits for ocular surface diagnostic tests, as well as collection and study of tears and mucin, which is difficult to perform in small rodents (3). Negative aspects of this model include the outbred source of most dogs, their maintenance costs, and potential difficulties with receipt of animal care and use committee approval for experimental procedures on this species (3). Finally, it must also be emphasized that signs of dry eye tend to be considerably more severe in dogs than in humans. Hypertrophic and hyperemic conjunctiva, mucous filaments, and a thick persistent mucopurulent ocular discharge, corneal vascularization, corneal melanosis, and reoccurring ulcers, are not infrequent in canine dry eye (3).

The existing animal models of dry eye mimic different pathogenic mechanisms of KCS, but at the moment none of them seems to mirror precisely the complexity and chronicity of this frequent and debilitating condition (3). Despite their small size, the advanced murine immunogenetics and extensive availability of reagents and knockout and transgenic strains make the mouse a very attractive model. Further studies incorporating both intrinsic (immune, endocrine, neuronal) and extrinsic (environmental) factors in dry eye pathogenesis in the mouse will offer important advances in the field (3).

New Scopolamine-Induced Dry Eye Model in Rats

Dry eye was induced in six week old female Lewis rats by a systemic and continuous delivery of scopolamine via osmotic pumps implanted subcutaneously.

Daily scopolamine doses of 12.5 mg and 25 mg applied for a 28-day period induced keratitis, a decrease in Muc5AC immunostaining density in the conjunctival epithelium, and modifications in the fatty acid composition of the exorbital lacrimal gland. Animals treated with a 12.5-mg/day dose of scopolamine exhibited an increase in corneal fluorescein staining after 2, 10, and 28 days. All animals exhibited unilateral or bilateral keratitis after 17 days. In the conjunctival epithelium, a significant decrease in Muc5AC immunostaining density was observed at early and late time points, and MHC II expression tended to be increased after 1, 7, 10, and 28 days, without reaching statistical significance. The levels of TNF-α, IL-1β and IL-6 mRNA were increased with scopolamine treatment in both conjunctiva and exorbital LG. This systemic and continuous scopolamine-induced model of dry eye in the rat may represent a helpful tool to investigate moderate dry eye (1).

Selected Dry Eye Model

The scopolamine-induced dry eye model was selected for this study due to the effectiveness of scopolamine in mimicking the symptoms of dry eye and the methods that were used to evaluate clinical signs of dry eye. Scopolamine was used as the induction article and its function is to induce a pharmacologic blockade of cholinergic (muscarinic) receptors in the lacrimal gland and therefore to decrease aqueous production (3). It has been demonstrated that scopolamine has a high selectivity for the muscarinic receptor, although it has been reported that high doses of scopolamine will also block nicotinic receptors. Since scopolamine has no preference for one of the different muscarinic subtypes, scopolamine will block the effects of acetylcholine at the muscarinic receptor throughout the body and brain and affect various physiological functions (43). Scopolamine was administered systemically via an Alzet® osmotic

pump (Model 2ML4) implanted subcutaneously for 28 days at 12.5 mg/day. The osmotic pump was used for a number of reasons. Mainly because it is small enough to use in rats and allows for targeted delivery of test article to virtually any tissue. It ensures around-the-clock exposure to test agents at predictable levels as well as provides a convenient method for the chronic dosing of laboratory animals. It minimizes unwanted experimental variables and ensures reproducible, consistent results. It also eliminates the need for nighttime or weekend dosing which in turn reduces handling and stress to laboratory animals. An added bonus is that it is a cost-effective research tool (44).

For Phase I, one treatment group of 5 female rats was administered scopolamine at a dose level of 12.5 mg/day. One group of 5 animals served as a control and was administered saline. One additional group of 3 animals served as a control and was not administered the scopolamine nor saline. Scopolamine and saline were administered continuously over 28 days via a subcutaneously implanted Alzet® osmotic pump at a dose level of 12.5 mg/day. Ocular assessments, including tear volume, fluorescein corneal staining, and corneal thickness measurements by ocular coherence tomography (OCT), were conducted on Days 0, 2, 7, 14, 21, and 28 (see Table 1).

Group	Number	Scopolamine Induction (Osmotic Pumps Implanted on Day 0)	Dose; Duration	Ocular Assessments	Termination
1	5	No pump implantations	Not Applicable	Days 0, 2, 7, 14, 21 and 28	Day 28
2	5	Pumps implanted/saline delivered	Not Applicable	Days 0, 2, 7, 14, 21 and 28	Day 28
3	5	Pumps implanted/scopolamine delivered	12.5 mg/day;28 Days	Days 0, 2, 7, 14, 21 and 28	Day 28

Table 1
Phase I: Establishment

For Phase II, four treatment groups of 5 female rats each were administered

scopolamine at a dose level of 12.5 mg/day. One additional group of 3 animals served as the control and was not administered scopolamine. Scopolamine was administered continuously over 28 days via a subcutaneously implanted Alzet® osmotic pump at a dose level of 12.5 mg/day. The vehicle control, saline eye drops, and positive control articles, Restasis® and Fluormetholone, were administered to three of the four induced groups beginning on Day 0. The vehicle and positive control articles were administered topically into both eyes at a dose volume of 50 µL per eye two times daily for 28 days. One of the induced groups served as the control and was not administered the vehicle nor positive control articles. Ocular assessments, including tear volume, fluorescein corneal staining, and corneal thickness measurements by OCT, were conducted on Days -2, 2, 7, 14, 21, and 28 (see Table 2).

Group	Number	Scopolamine Induction	Dose; Duration	Treatment	Route; Schedule	Ocular Assessments	Termination
5	5	No pumps Implanted	Not Applicable	No	Not Applicable	Pretest and Days 2, 7, 14, 21, and 28	Day 28
6	5	Yes	12.5 mg/day; 28 days	No	Not Applicable		
7	5	Yes	12.5 mg/day; 28 days	Saline eye drops	Topical ocular; Twice daily		
8	5	Yes	12.5 mg/day; 28 days	Restasis	Topical ocular; Twice daily		
9	5	Yes	12.5 mg/day; 28 days	FML	Topical ocular; Twice daily		

Table 2
Phase II: Validation

The main objective of this study is to understand the unique characteristics of dry eye and its limitations to help provide further insight into the development of more effective therapeutic solutions (3). This study will establish the dry eye condition, identify symptoms of dry eye using ocular imaging, and confirm that healing can be seen after application of topical medications available to treat dry eye. Previous studies have indicated that scopolamine is an effective way of inducing the dry eye condition by blocking muscarinic receptors that innervate the lacrimal functional unit and interrupting the physiological processes that maintain the tear film at the ocular surface (3). This study also builds upon that research by eliminating variables introduced by genetically engineered and knockout strains of rats as well as tests the efficacy of available drugs, such as Restasis, to treat the condition. The results of this study will provide proven diagnostic procedures to identify clinical dry eye, which topical therapies are most effective in treating the condition, and make a contribution in the field of dry eye study.

MATERIALS AND METHODS

Facilities

All research for these studies were conducted at MPI Research in Mattawan, MI.

Animals

All research conducted for these studies were compliant with all applicable regulations governing the care and use of laboratory animals. Animal welfare for this study was in compliance with the United States Department of Agriculture's (USDA) Animal Welfare Act (Title 9 Code of Federal Regulations [CFR] Parts 1,2, and 3). The Guide for the Care and Use of Laboratory Animals, Institute of Laboratory Animal Resources, National Academy Press, Washington, D.C., 1996, were followed. The facility maintains an Animal Welfare Assurance statement with National Institutes of Health, Office of Laboratory Animal Welfare. The study protocol and all necessary amendments were reviewed and approved by the Institutional Animal Care and Usage Committee (IACUC) before animal receipt or transfer.

Approximately six-week-old female Lewis rats (Charles River Laboratories) weighing at least 150 grams were used for each phase of this study. Female rats were used because dry eye is a condition predominantly seen in women and at around six weeks is when a rat reaches sexual maturity (1). Rats of this age were also used because the study that this is modeled after by Viau. *et. al.* (2008), used six-week-old rats. Animals were housed in animal quarters under controlled temperature (22±1°C), light conditions (12-hour light/12-hour dark cycle), and humidity (55-60%), with

water and food available ad libitum.

Filling of Osmotic Pumps

Induction of dry eye was accomplished by cholinergic blockade using scopolamine which was continuously and systemically administered to the animals via Alzet® osmotic pumps (Model 2ML4) for 28 days. The induction article, scopolamine hydrobromide, was solubilized at MPI Research by sonication and heating to approximately 35°C. Scopolamine has been used in previous experiments and proven to induce moderate dry eye in rats (1,2). Prior to surgical implantation of the osmotic pumps, the induction article needed to be placed into the pumps via a filling tube or syringe. All filling of pumps were conducted in a sterile environment via a laminar flow hood (Labconco Purifier Class II Biosafety Cabinet). Each pump was weighed empty (Mettler Toledo ML Model Analytical Balance) in a sterile, metal petri dish and the value was recorded (data not shown). The flow moderator was removed before filling. Using a three milliliter (mL) syringe, the test article or vehicle was drawn up and attached to a blunt-tipped 25-gauage filling tube. The osmotic pump was held upright and the filling tube was inserted through the opening at the top of the pump until it could go no further. The plunger of the syringe was slowly pushed until the test material appeared in the opening and then filling stopped. The filling tube was removed, the overflow fluid was wiped off, the flow moderator was repositioned in the pump, and the filled pump was weighed. An empty weight was recorded because in order for the pump to work effectively, the fill volume should be over 90% of the total fill volume for each pump. The volume and pump delivery rate differ among lots.

Implantation of Osmotic Pumps

Prior to subcutaneous surgical implantation of osmotic pumps, the animals were placed in anesthesia chambers connected to isoflurane (Abbott IsoFlo®, Isoflurane, USP) via VetEquip Precision Vaporizer hooked up to an oxygen source. Anesthesia was monitored by pinna reflex, pedal reflex, and corneal blink reflexes. Eye lubricant, a sodium chloride eye drop solution, was applied to the eyes during anesthesia and surgery. The implant site was the dorsal scapular region of the animal. Aseptic technique was strictly adhered to during surgery as well as pre- and post-operation to assure the animals did not get an infection. The implant site was shaved, cleaned using chlorhexidine solution, and 70% alcohol for sterilization before surgery. An incision was made in the scapular region and a space slightly bigger than the pump was created under the skin using a dull surgical instrument that will not lacerate, puncture, or injure any surrounding tissue. The pump was placed subcutaneously in the space with the flow moderator facing away from the incision. The incision was closed with a synthetic, absorbable suture made of polyglycolic acid and surgical sealant. The animals were placed in their cages post-operation and monitored to ensure recovery and overall health. Cageside observations were conducted twice daily to observe the overall health of animals and to ensure that water and food were readily available to the animals throughout the study.

Phase I: Establishment

This study phase included a normal control group of animals without implanted pumps (n = 3) and a second control group of animals with pumps delivering vehicle (n = 5). A third group of animals (n = 5) induced with scopolamine will also be included (Refer to Table 1). The Alzet® model 2ML4 (lot number 10232-09) delivery rate is

2.5 µL/hour. Two extra animals were ordered to assure healthy animals were available for the study. Thus, a total of 15 female Lewis rats were used for this phase of the study.

Phase II: Validation

This phase included two negative control groups including a group without pump implantations and a group with pump implantations but received saline solution instead of scopolamine. A third control group was implanted with pumps delivering scopolamine and treated with the topical vehicle, saline solution. The fourth group of animals was implanted with pumps delivering scopolamine and treated with Restasis®, a commercially available dry eye medication, while the remaining group was implanted with pumps delivering scopolamine and treated with a commercial product containing dexamethasone. Dexamethasone is a corticosteroid. It is a long-acting analog that has minimal mineralocorticoid activity and maximal anti-inflammatory activity. Its primary use is to induce strong anti-inflammatory therapy acutely (45). The osmotic pump delivery rate was 2.80 µL/hr, based on the manufacturer's supplied information for this lot of pumps. Fluorometholone (FML) was the selected corticosteroid and was used as secondary steroidal anti-inflammatory medication. The saline eye drops, Restasis®, and FML were dosed on Days 0-28 (Refer to Table 2). All articles were administered with a micropipette at a volume of 50 microliters/eye/dose into both eyes of each animal. Three extra animals were ordered to assure healthy animals were available for the study. Thus, a total of 26 female Lewis rats were used for this phase of the study.

Clinical Examinations (All Phases)

The clinical signs of dry eye were evaluated by tear volume measurements with sterilized phenol-red thread (FCI Opthalmics Zone Quick™), corneal staining with 0.2% sodium fluorescein (Novartis Pharmaceutials), and corneal thickness.

The animals were anesthetized prior to ocular assessments using isoflurane vapors to effect. An integrated multi-patient anesthesia system (VetEquip IMPAC^6 Complete Anesthesia System) with isoflurane vaporizer attachment was used to sedate the animals prior to examination. Anesthesia was monitored by pinna reflex, pedal reflex, and/or corneal blink reflexes.

Tear Volume

Tear volume measurements were performed using phenol-red threads and recorded. A phenol-red impregnated thread will be applied to the ocular surface in the lateral canthus for at least thirty seconds.

The bottom eyelid was abducted from the eye using forceps and the thread was placed in the lateral canthus with blunt forceps. Once the thread was in the correct position, the bottom eyelid was released from the forceps and allowed to hold the thread in place for thirty seconds. The length of the wetted thread was measured using an included scale provided in millimeters.

Corneal Staining

Image Collection

Immediately following tear volume measurements, clinical signs of corneal dryness were evaluated utilizing fluorescein staining. One drop of 0.2% sodium

fluorescein was placed in the upper conjunctival sac of the right eye and allowed to impregnate the cornea. After two minutes, the eye was rinsed liberally with ophthalmic eye wash (0.9% saline). The cornea was then evaluated using photographic slit lamp under cobalt blue light (Heidelberg Engineering). To quantify the fluorescein impregnation, the cornea was observed using confocal scanning-laser ophthalmoscopy (cSLO) at 488 nm with a Heidelberg Retinal Angiograph (HRA) (Heidelberg Engineering). Corneal hydration was maintained with saline-type eye drops as needed. The Heidelberg cSLO was used under the following settings: 15°, 50 diopters (D), and sensitivity 50. Images were later exported in Joint Photographic Group (JPG) format for offline processing using ImageJ (National Institutes of Health) and Matlab software programs.

Image Processing

JPG images were opened in ImageJ and a predetermined ROI circle (area = 289,632 pixels) was placed and centered manually. All pixels outside the ROI were cleared and the altered image was saved (see Figure 1).

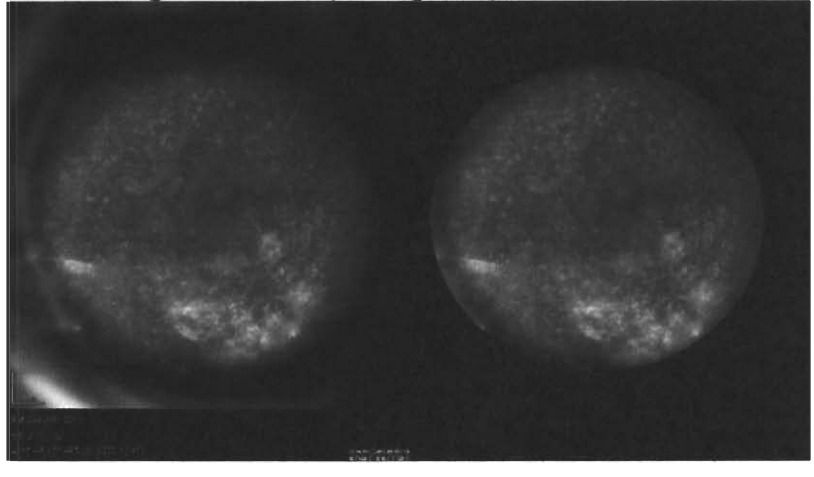

Figure 1 Example of Image Captured with the Heidelberg cSLO: Before (left) and after (right) subtraction of data outside of the ROI (scale bar in bottom left corner set at 200 μm)

Using Matlab, the background fluorescence haze was subtracted from the altered images (threshold = 50). The mean image intensity as well as the remaining area stained was calculated (sum of all non-zero pixels). The images were graded automatically using the scoring system suggested by Viau, *et.al.* (2008) (1), who also used the Heidelberg cSLO for corneal staining measurements. For each animal, the ratio of fluorescent-positive area to total area of the ocular surface was calculated on one picture, using Matlab in a masked fashion. The ratio was denoted as grade 0 when there was no staining, grade 0.5 when less than 5% was stained, grade 1 when less than 10% was stained, grade 2 when less than 20% was stained, grade 3 when less than 40% was stained, and grade 4 when 40% or more was stained (see Figure 2). The mean was also calculated for each group of animals.

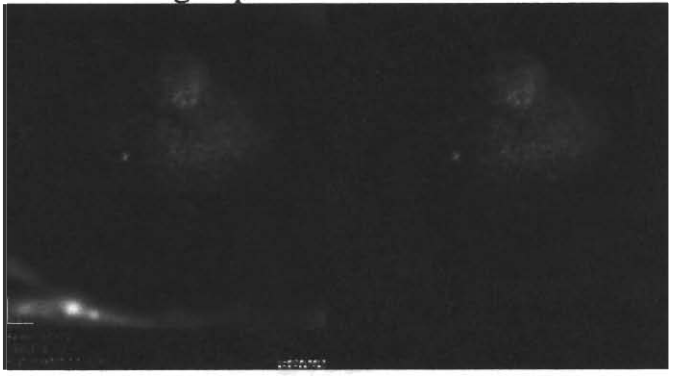

Score: 1

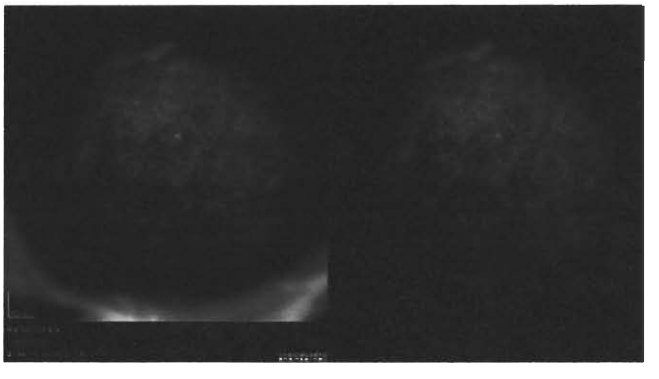

Score: 2

Score: 3

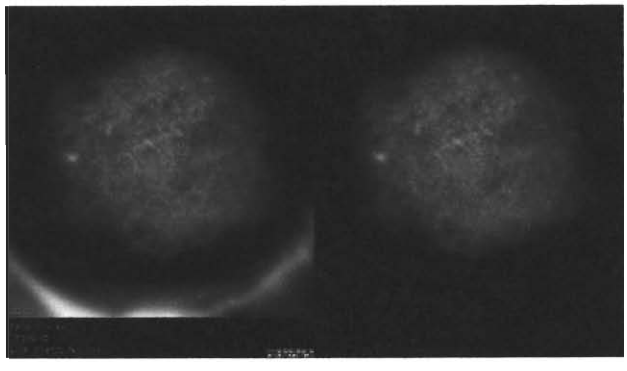

Score: 4

Figure 2 Examples of Corneal Staining Scores

Corneal Thickness

Corneal thickness was measured immediately following fluorescein corneal staining. OCT images of the central cornea were collected with the Heidelberg cSLO using an additional 80D lens, 30° viewing angle, and 40D camera focus. Images were exported using ImageJ and four land markers were noted allowing for measurement of the air-tear film-epithelium interface (1-2), epithelium (2-3), and stroma (3-4) (see Figure 3). Positions of markers were saved and thickness of each layer was measured in pixels and calculated using Matlab.

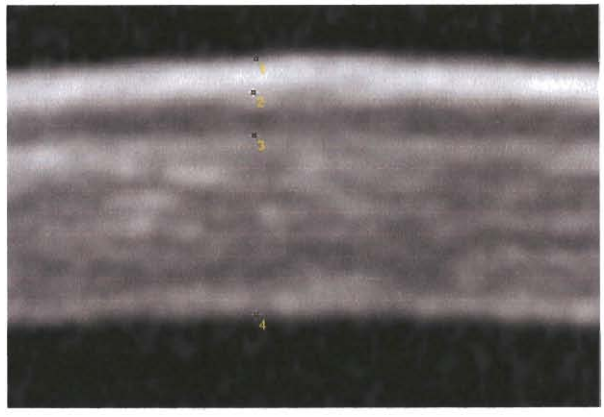

Figure 3 OCT with Placement of Markers

Euthanasia and Tissue Collection

All animals were euthanized via carbon dioxide inhalation and death was verified by exsanguination via the abdominal vena cava. The cornea, conjunctiva, and lacrimal gland were collected from the right eye of all animals at the end of each phase of the study. The harvested tissues were fixed in RNA*later*® solution (Life Technologies, Ambion) and refrigerated at 4°C for at least twenty-four hours before they were transferred to a -20°C freezer where they can be held indefinitely. These tissues were harvested for future molecular testing.

Statistics

Statistical analysis will be performed using ANOVA and calculated using Matlab and MiniTab. *P* values of less than 0.05 were considered statistically significant. Grouping information using the Tukey method was used to determine significant difference among groups.

RESULTS

Phase I: Establishment

Tear Volume

The objective of this experiment was to see if tear production was reduced in the group being administered scopolamine as compared to the control/untreated group and the group being administered saline. A shorter wetted thread length would indicate low tear production and a longer wetted thread length would indicate high tear production. Results of tear volume measurements of control animals, animals implanted with saline- and scopolamine-filled pumps are illustrated in Figure 4.

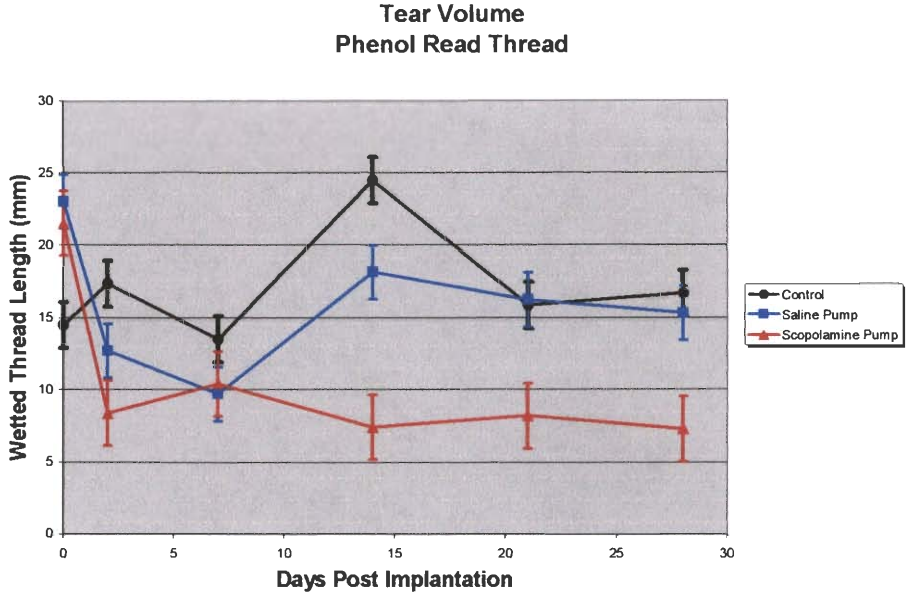

Figure 4 Phase I: Tear Volume as Measured Using Wetted Zone Quick Phenol-Red Thread

The results in Figure 4 indicate that there is a reduction in tear volume in the

scopolamine treated group. At the beginning of the experiment on Day 0, the average wetted thread length for this group was approximately 21 mm while at the end of the experiment on Day 28, the average wetted thread length was 7.3 mm. One-way ANOVA was run using MiniTab and $P = 0.000$ was calculated which indicates statistical significance among the groups. Grouping information using the Tukey method was used to determine significant difference among groups (see Table 3).

	N	Mean	Grouping*
Control	36	17.056	A
Saline	60	15.833	A
Scopolamine	60	10.533	B

*Means that do not share a letter are significantly different.

Table 3

Grouping Information Using Tukey Method: Phase I - Tear Volume (mm)

As indicated by the Tukey calculations, there was a significant difference between the control and saline groups as compared to the scopolamine treated groups. The results from this experiment indicate that tear volume was reduced in the scopolamine treated groups.

Corneal Staining

Immediately following tear volume measurements, clinical signs of corneal dryness were evaluated utilizing fluorescein staining. One drop of 0.2% sodium fluorescein was placed in the upper conjunctival sac of the right eye and allowed to impregnate the cornea. The cornea was then evaluated using photographic slit lamp under cobalt blue light (Heidelberg Engineering). To quantify the fluorescein impregnation, the cornea was observed using confocal scanning-laser ophthalmoscopy (cSLO) at 488 nm with a Heidelberg Retinal Angiograph (HRA) (Heidelberg Engineering). JPG images were opened in ImageJ and a predetermined ROI circle

(area = 289,632 pixels) was placed and centered manually. All pixels outside the ROI were cleared and the altered image was saved as shown in Figure 1. Using Matlab, the background fluorescence haze was subtracted from the altered images (threshold = 50). The mean image intensity as well as the remaining area stained was calculated (sum of all non-zero pixels). The images were graded automatically using the scoring system suggested by Viau, *et.al.* (2008), who also used the Heidelberg cSLO for corneal staining measurements (1). For each animal, the ratio of fluorescent- positive area to total area of the ocular surface was calculated on one picture, using Matlab in a masked fashion. The ratio was denoted as grade 0 when there was no staining, grade 0.5 when less than 5% was stained, grade 1 when less than 10% was stained, grade 2 when less than 20% was stained, grade 3 when less than 40% was stained, and grade 4 when 40% or more was stained. Results of corneal staining measurements of control animals, animals implanted with saline- and scopolamine-filled pumps are illustrated in Figure 5.

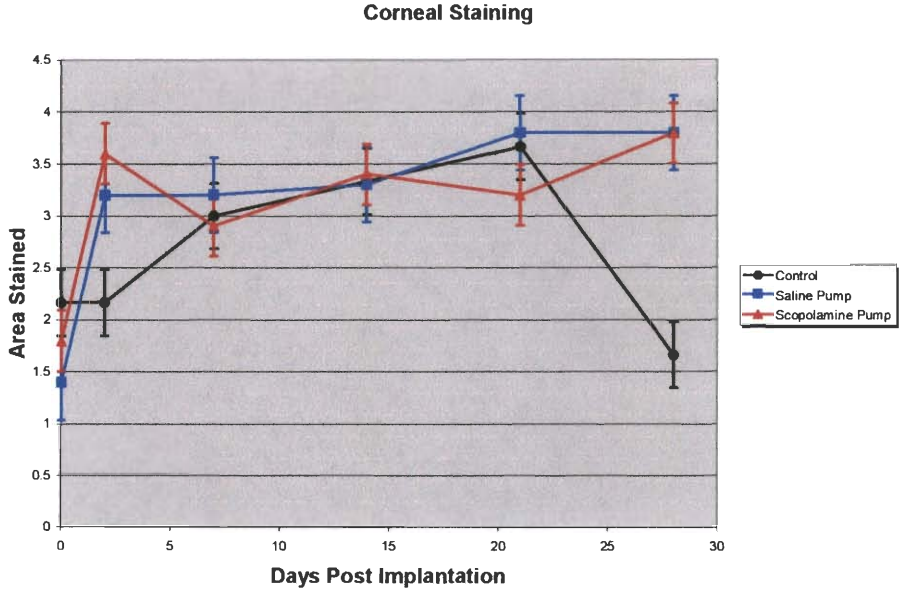

Figure 5 Phase I: Corneal Staining Measurements for All Groups across All Time Points with "Area Stained" Based on Scale Rating of 1-4

Corneal staining increased from about 1.5 – 2 in all groups to about 4 as the study progressed and there was no difference in groups until Day 28 where the control group seemed to spontaneously recover to around 1.5 as seen in Figure 5. One-way ANOVA was run using MiniTab and $P = 0.235$ was calculated which indicates that there was no statistical significance among the groups. Grouping information using the Tukey method was used to determine significant difference among groups (see Table 4).

	N	Mean	Grouping*
Control	18	84,900	A
Saline	30	110,681	A
Scopolamine	30	115,532	A

*Means that do not share a letter are significantly different.

Table 4

Grouping Information Using Tukey Method: Phase I - Corneal Staining (pixels)

As indicated by the Tukey calculations, there was no significant difference among the groups. The results from this experiment indicate that although there was a tendency toward increased corneal staining among the groups, there was no actual significant difference among the groups.

Corneal Thickness

Corneal thickness was measured immediately following fluorescein corneal staining. OCT images of the central cornea were collected with the Heidelberg cSLO using an additional 80D lens, 30° viewing angle, and 40D camera focus. Images were exported using ImageJ and four land markers were noted allowing for measurement of the air-tear film-epithelium interface (1-2), epithelium (2-3), and stroma (3-4) as illustrated in Figure 3. This experiment was designed to determine if there is a relationship between corneal thickness and dry eye. For instance, I expected that

corneal thickness would increase over the 28 day study in the scopolamine treated group whereas the control group should have relatively no change in corneal thickness over the course of the study.

The results of the tear film – epithelium interface thickness measurements among all groups are illustrated in Figure 6.

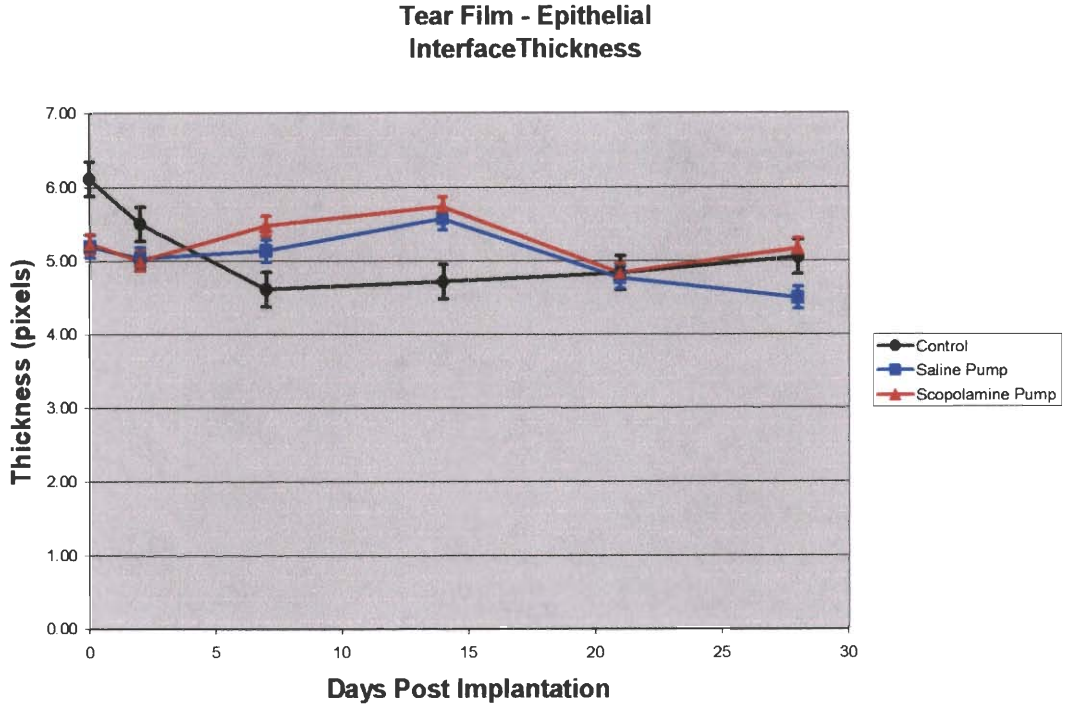

Figure 6 Phase I: Tear Film – Epithelial Interface Thickness Measurements

As shown in the figure above, the tear film – epithelium interface thickness was between 5 and 6 pixels for all groups at the beginning of the experiment and between 4.5 and 5 pixels at the end of the experiment. This is a very small change. One-way ANOVA was run using MiniTab and $P = 0.676$ was calculated which indicates that there was no statistical significance among the groups. Grouping information using the Tukey method was used to determine significant difference among groups (see Table 5).

	N	Mean	Grouping*
Control	18	5.1394	A
Saline	30	5.0337	A
Scopolamine	30	5.2410	A

*Means that do not share a letter are significantly different.

Table 5

Grouping Information Using Tukey Method: Phase I - Corneal Thickness – Tear Film/Epithelium Interface (pixels)

As indicated by the Tukey calculations, there was no significant difference among the groups. The results from this experiment indicate that there was no significant change in tear film – epithelium interface thickness.

The results of the epithelium thickness measurements among all groups are illustrated in Figure 7.

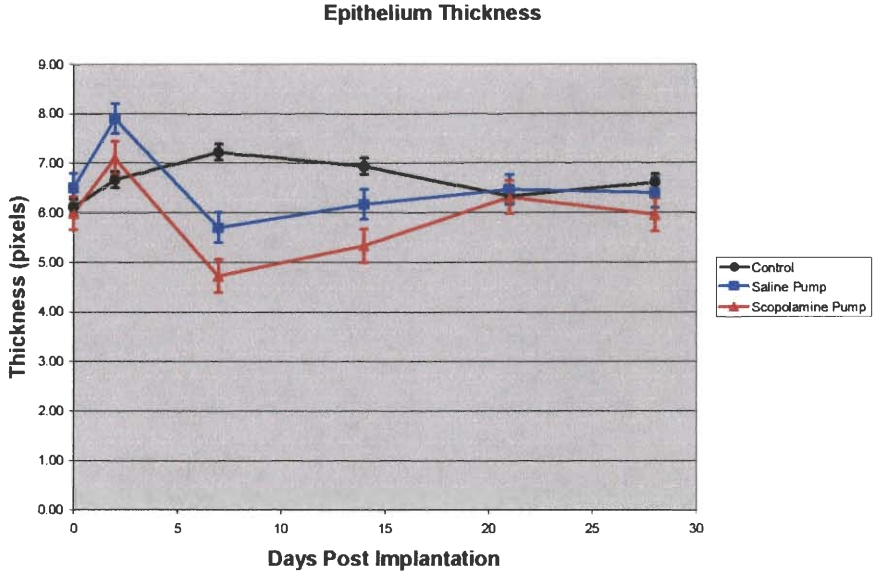

Figure 7 Phase I: Epithelium Thickness Measurements

As shown in the figure above, the epithelium thickness was between 6 and 6.5 pixels for all groups at the beginning of the experiment. The scopolamine groups decreased to about 4.5 pixels over the next two time points but recovered at the end of the study and finished at about the same thickness as the beginning of the study. One-

way ANOVA was run using MiniTab and P = 0.029 was calculated which indicates that there was statistical significance among the groups. Grouping information using the Tukey method was used to determine significant difference among groups (see Table 6).

	N	Mean	Grouping*
Control	18	6.649	A
Saline	30	6.521	A
Scopolamine	30	5.906	A

*Means that do not share a letter are significantly different.

Table 6

Grouping Information Using Tukey Method: Phase I - Corneal Thickness – Epithelium (pixels)

As indicated by the Tukey calculations, there was no significant difference among the groups. The results from this experiment indicate that the statistical significance could be due to the drop in the epithelium thickness at Day 7 and Day 14 but throughout the course of the study the epithelium thickness was about the same for all groups.

The results of the stroma thickness measurements among all groups are illustrated in Figure 8.

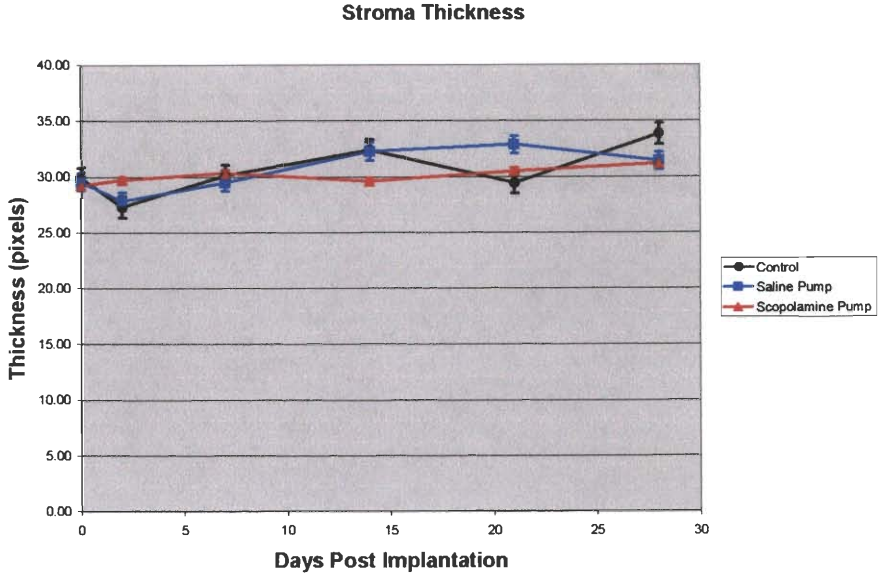

Figure 8 Phase I: Stroma Thickness Measurements

As shown in the figure above, the stroma thickness was around 30 pixels for all groups at the beginning of the experiment and between 30 and 30.5 pixels at the end of the experiment. This is a very small change. One-way ANOVA was run using MiniTab and $P = 0.664$ was calculated which indicates that there was no statistical significance among the groups. Grouping information using the Tukey method was used to determine significant difference among groups (see Table 7).

	N	Mean	Grouping*
Control	18	30.506	A
Saline	30	30.577	A
Scopolamine	30	30.093	A

*Means that do not share a letter are significantly different.

Table 7

Grouping Information Using Tukey Method: Phase I - Corneal Thickness – Stroma (pixels)

As indicated by the Tukey calculations, there was no significant difference among the groups. The results from this experiment indicate that there was no

significant change in stroma thickness over the course of the study.

Phase II: Validation

Tear Volume

The objective of this experiment was to see if tear production was reduced in the groups being administered scopolamine (one group not receiving treatment, one group being treated with Restasis, and one group being treated with FML) as compared to the control group. A shorter wetted thread length would indicate low tear production and a longer wetted thread length would indicate high tear production. Results of tear volume measurements all groups are illustrated in Figure 9.

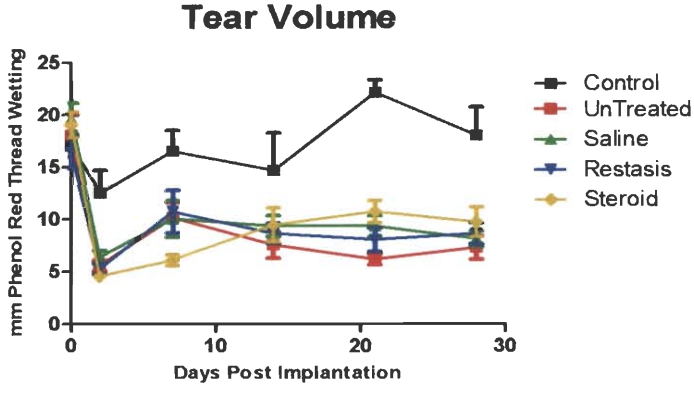

Figure 9 Phase II: Tear Volume as Measured Using Wetted Zone Quick Phenol-Red Thread (mm)

The results in Figure 9 indicate that there is a reduction in tear volume in all groups except the control group. At the beginning of the study on Day 0, the average wetted thread length for all groups was approximately between 15 mm and 20 mm. At the end of the study on Day 28, the average wetted thread length of the scopolamine-treated groups was between 5 mm and 10 mm while the control group was still around .

20 mm. One-way ANOVA was run using MiniTab and $P = 0.000$ was calculated which indicates statistical significance among the groups. Grouping information using the Tukey method was used to determine significant difference among groups (see Table 8).

	N	Mean	Grouping*
Control	36	16.806	A
Scopolamine Untreated	48	8.8333	B
Saline Eye Drops	60	10.450	B
Restasis Eye Drops	60	9.600	B
FML Eye Drops	60	9.917	B

*Means that do not share a letter are significantly different.

Table 8

Grouping Information Using Tukey Method: Phase II - Tear Volume (mm)

As shown by the Tukey calculations, there was a significant difference between the control group and the scopolamine treated groups. The results from this experiment indicate that tear volume was reduced in the scopolamine treated groups.

Corneal Staining

Immediately following tear volume measurements, clinical signs of corneal dryness were evaluated utilizing fluorescein staining. One drop of 0.2% sodium fluorescein was placed in the upper conjunctival sac of the right eye and allowed to impregnate the cornea. The cornea was then evaluated using photographic slit lamp under cobalt blue light (Heidelberg Engineering). To quantify the fluorescein impregnation, the cornea was observed using confocal scanning-laser ophthalmoscopy (cSLO) at 488 nm with a Heidelberg Retinal Angiograph (HRA) (Heidelberg Engineering). JPG images were opened in ImageJ and a predetermined ROI circle (area = 289,632 pixels) was placed and centered manually. All pixels outside the ROI were cleared and the altered image was saved as shown in Figure 1. Using Matlab, the

background fluorescence haze was subtracted from the altered images (threshold = 50). The mean image intensity as well as the remaining area stained was calculated (sum of all non-zero pixels). The images were graded automatically using the scoring system suggested by Viau, *et.al.* (2008), who also used the Heidelberg cSLO for corneal staining measurements. For each animal, the ratio of fluorescent- positive area to total area of the ocular surface was calculated on one picture, using Matlab in a masked fashion. The ratio was denoted as grade 0 when there was no staining, grade 0.5 when less than 5% was stained, grade 1 when less than 10% was stained, grade 2 when less than 20% was stained, grade 3 when less than 40% was stained, and grade 4 when 40% or more was stained. Results of corneal staining measurements pertaining to area stained for all groups are illustrated in Figure 10.

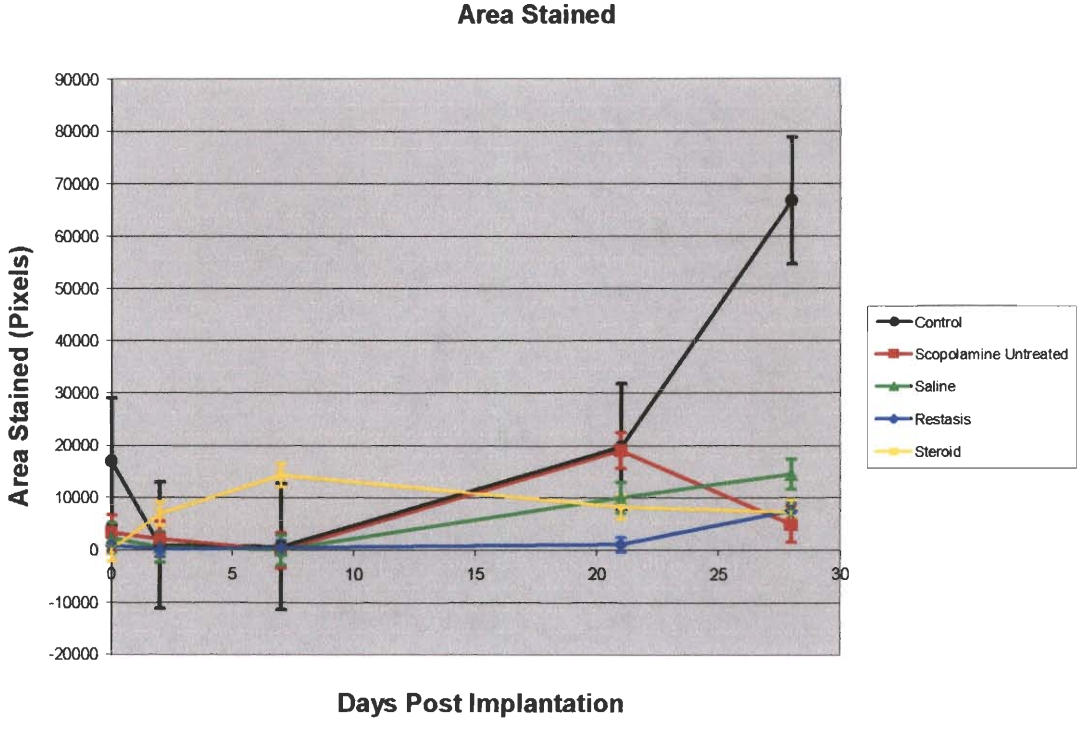

Figure 10 Phase II: Area Stained of Cornea in Pixels

All values for Day 14 were excluded from the data set due to inconsistent

scoring among all groups. With the data from Day 14 excluded, corneal staining among the groups treated with scopolamine were very similar throughout the study. Corneal staining in the control group seemed to remain fairly consistent until the last two weeks of the study where the staining spontaneously increased to around 65,000 pixels as seen in Figure 10. One-way ANOVA was run using MiniTab and $P = 0.050$ was calculated which indicates that there was no statistical significance among the groups. Grouping information using the Tukey method was used to determine significant difference among groups (see Table 9).

	N	Mean	Grouping*
Control	15	21,015	A
Scopolamine Untreated	22	5,640	A B
Saline Eye Drops	25	5,540	A B
Restasis Eye Drops	25	2,084	B
FML Eye Drops	25	5,540	A B

*Means that do not share a letter are significantly different.

Table 9

Grouping Information Using Tukey Method: Phase II - Corneal Staining – Area Stained (pixels)

As indicated by the Tukey calculations, there was a significant difference among the control group and the scopolamine group treated with Restasis drops. Also, the results from the Tukey calculations indicate that there were similar corneal staining amongst the scopolamine untreated group and scopolamine groups treated with saline and FML drops. However, these three groups also shared similar statistical significance with the control group as well as the scopolamine group treated with Restasis drops. The results from this experiment indicate that there were inconsistent results measuring corneal staining area.

Scoring results of corneal staining measurements for all groups are illustrated in Figure 11.

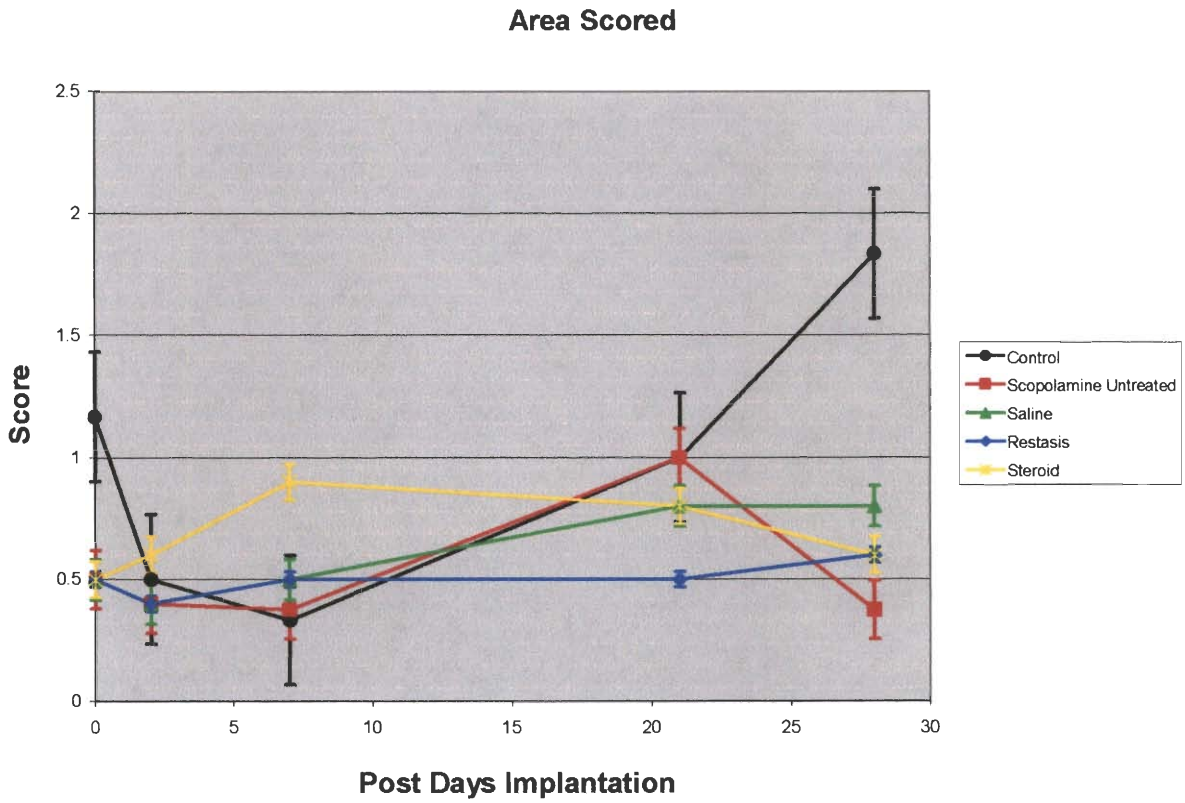

Figure 11 Phase II: Scoring Results of Corneal Staining

All values for Day 14 were excluded from the data set due to inconsistent scoring among all groups. With the data from Day 14 excluded, corneal staining among the groups treated with scopolamine was very similar throughout the study. Corneal staining in the control group seemed to remain fairly consistent until the last two weeks of the study where the staining spontaneously increased to a score of around 2 as seen in Figure 11. One-way ANOVA was run using MiniTab and $P = 0.128$ was calculated which indicates that there was no statistical significance among the groups. Grouping information using the Tukey method was used to determine significant difference among groups (see Table 10).

	N	Mean	Grouping*
Control	15	0.9667	A
Scopolamine Untreated	22	0.5682	A
Saline Eye Drops	25	0.6000	A
Restasis Eye Drops	25	0.5000	A
FML Eye Drops	25	0.6800	A

*Means that do not share a letter are significantly different.

Table 10

Grouping Information Using Tukey Method: Phase II - Corneal Staining – Area Scored

As indicated by the Tukey calculations, there was no significant difference among the groups. The results from this experiment indicate that there was no significant difference in regards to corneal staining scores among the test groups.

Corneal Thickness

Corneal thickness was measured immediately following fluorescein corneal staining. OCT images of the central cornea were collected with the Heidelberg cSLO using an additional 80D lens, 30° viewing angle, and 40D camera focus. Images were exported using ImageJ and four land markers were noted allowing for measurement of the air-tear film-epithelium interface (1-2), epithelium (2-3), and stroma (3-4) as illustrated in Figure 3. This experiment is trying to see if there is a relationship between corneal thickness and dry eye. For instance, it would be expected that corneal thickness would increase over the 28 day study in the scopolamine-untreated group whereas the control group should have relatively no change in corneal thickness over the course of the study.

The results of the tear film – epithelium interface thickness measurements among all groups are illustrated in Figure 12.

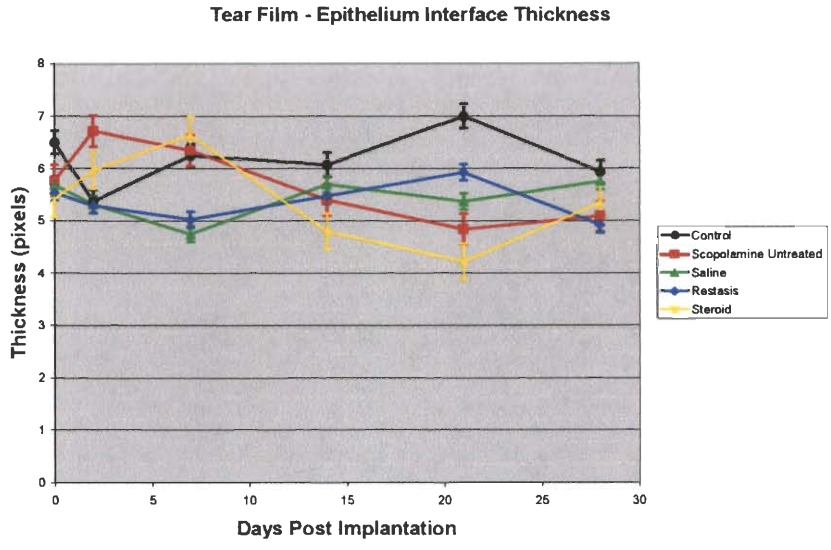

Figure 12 Phase II: Tear Film – Epithelial Interface Thickness Measurements

As shown in the figure above, the tear film – epithelium interface thickness measurements were up and down for all groups throughout the course of the study. One-way ANOVA was run using MiniTab and $P = 0.073$ was calculated which indicates that there was no statistical significance among the groups. Grouping information using the Tukey method was used to determine significant difference among groups and shown in Table 11.

	N	Mean	Grouping*
Control	18	6.189	A
Scopolamine Untreated	26	5.742	A
Saline Eye Drops	30	5.433	A
Restasis Eye Drops	30	5.367	A
FML Eye Drops	30	5.401	A

*Means that do not share a letter are significantly different.

Table 11

Grouping Information Using Tukey Method: Phase II - Corneal Thickness – Tear Film/Epithelium Interface (pixels)

As indicated by the Tukey calculations, there was no significant difference

among the groups. The results from this experiment indicate that there was no significant change in tear film – epithelium interface thickness.

The results of the epithelium thickness measurements among all groups are illustrated in Figure 13.

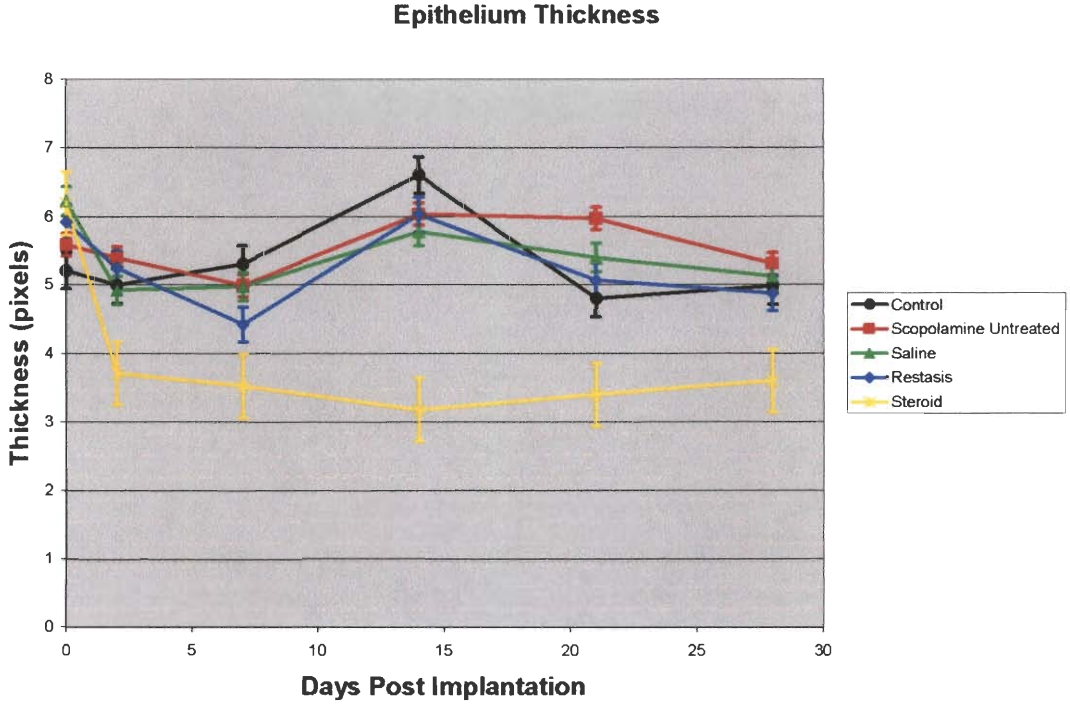

Figure 13 Phase II: Epithelium Thickness Measurements

As shown in the figure above, the epithelium thickness reduces sharply on Day 2 and stays between 3-4 pixels thick for the remainder of the study. This is in contrast to the rest of the groups who remain between 5-6 pixels throughout the study. One-way ANOVA was run using MiniTab and $P = 0.000$ was calculated which indicates that there was statistical significance among the groups. Grouping information using the Tukey method was used to determine significant difference among groups and (see Table 12).

	N	Mean	Grouping*
Control	18	5.318	A
Scopolamine Untreated	26	5.547	A
Saline Eye Drops	30	5.406	A
Restasis Eye Drops	30	5.262	A
FML Eye Drops	30	3.935	B

*Means that do not share a letter are significantly different.

Table 12

Grouping Information Using Tukey Method: Phase II - Corneal Thickness – Epithelium (pixels)

As indicated by the Tukey calculations, there was a significant difference between the FML-treated group when compared to all other groups on study. The results from this experiment indicate that FML has an effect on the thickness of the corneal epithelium and more specifically results in a thinning of the epithelium.

The results of the stroma thickness measurements among all groups are illustrated in Figure 14.

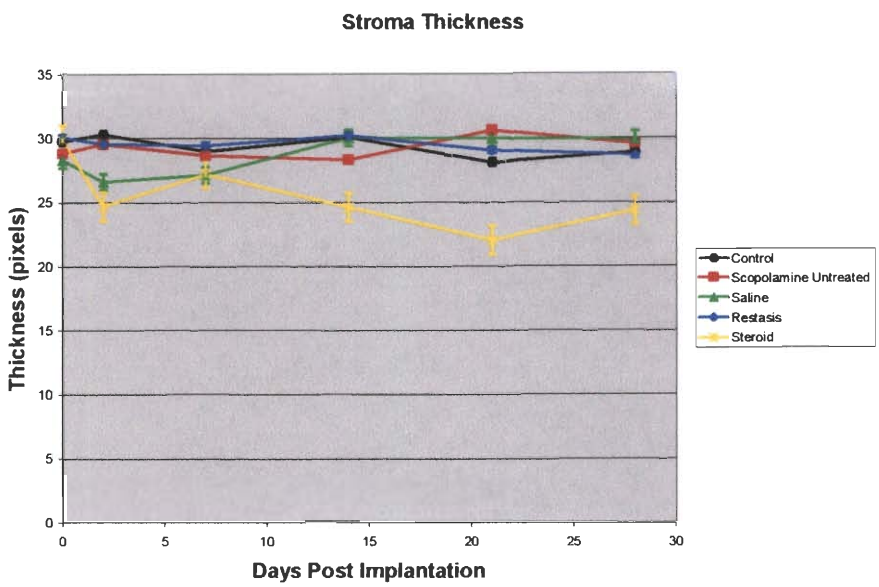

Figure 14 Phase II: Stroma Thickness Measurements

As shown in the figure above, the stroma thickness was around 30 pixels for all groups except throughout the study except for the steroid-treated group. The steroid-treated group started at 30 pixels and decreased to about 24 pixels by the end of the study. One-way ANOVA was run using MiniTab and $P = 0.001$ was calculated which indicates that there was statistical significance among the groups. Grouping information using the Tukey method was used to determine significant difference among groups (see Table 13).

	N	Mean	Grouping*
Control	18	29.489	A
Scopolamine Untreated	26	29.532	A
Saline Eye Drops	30	29.246	A
Restasis Eye Drops	30	28.649	A
FML Eye Drops	30	25.455	B

*Means that do not share a letter are significantly different.

Table 13

Grouping Information Using Tukey Method: Phase II - Corneal Thickness – Stroma (pixels)

As indicated by the Tukey calculations, there was a significant difference between the FML-treated group when compared to all other groups on study. The results from this experiment indicate that FML has an effect on the thickness of the stroma and more specifically results in a thinning of the stroma.

DISCUSSION

In Phase I, animals receiving scopolamine had a reduction in tear volume as early as 2 days after pump implantation and saline treated or control animals did not have similar tear reduction. All groups had increased corneal staining and there was no significant difference in corneal thickness between groups. While tear production was decreased in animals that received scopolamine, corneal staining was significantly increased in all animals on study. Corneal thickness is not commonly reported in dry eye exams, but studies where this has been reported have seen a thinning of the cornea with dry eye severity (46). Since all animals had increased corneal staining, future studies should include a validation study to determine if treatment with Restasis, FML, or saline will alleviate dry eye symptoms.

In Phase II, the model was validated using topical saline, steroid, or Restasis. All groups receiving scopolamine via osmotic pump had a reduction in tear volume within five days. Tear volume did not increase over the course of the study which indicates that the saline drops, Restasis, and steroid were not successful in recovering tear production. There was no significant difference among control and test groups in the corneal staining assessments.

This study demonstrated continuous systemic administration of scopolamine to female Lewis rats and resulted in reduced tear volumes as measured during the 28 days following pump implantations. Thinning of the epithelium and stroma of the steroid-treated group indicates that dry eye was evident in Phase II, however, FML may not be as effective of a treatment as compared to saline drops or Restasis. FML caused the inflammatory response to decrease but it also may have caused important

biological functions in the corneal cells to cease such as a quick turnover rate which could contribute to the thinning and pathogenesis seen in dry eye. Fluorescein corneal staining was increased, although high inter-animal variability prohibited definitive group comparisons. For example, on Day 14 the animals receiving Restasis treatment had a spike in their corneal staining score to about 2 but decreased back to a score of 0.5 on Day 21. Looking at the data, all animals in that group averaged a score of about 0.5 for the duration of the study except on Day 14; three animals had scores of 2, 3, and 4, respectively, which skewed the results. If more animals were on study, these outliers would not have had as great of an impact on the data and altering of the results. The data is shown below in Table 10 with outliers highlighted in red.

	Day 0	**Day 2**	**Day 7**	**Day 14**	**Day 21**	**Day 28**
4014	0.5	0.5	0.5	**4**	0.5	0.5
4015	0.5	0.5	0.5	**3**	0.5	1
4016	0.5	0.5	0.5	0.5	0.5	0.5
4017	0.5	0.5	0.5	1	0.5	0.5
4018	0.5	0	0.5	**2**	0.5	0.5
Average Score	**0.5**	**0.4**	**0.5**	**2.1**	**0.5**	**0.6**

Table 14
Scores of Corneal Staining in Phase II Restasis Treated Groups

Environmental factors also need to be taken into consideration when looking at the corneal staining data. The urea levels from urine could play a factor in corneal staining. Higher levels of urea could have a significant factor in affecting tear film homeostasis. The bedding that the rats had in their cages may have played a factor in the highly variable corneal staining scores because it could have scratched their eyes and contributed to higher urea levels. The cages should be swapped out for metabolism cages in future studies so that all of the feces and urine would be collected outside of the cage and all environmental factors such as temperature and humidity

could be completely controlled.

This study is a step in the right direction as far as studying the acute effects of dry eye and to discover the best ways to diagnose and treat the condition. However, it is limited in the length of time you can actually study the animals because the osmotic pumps only have 28 days of scopolamine administration. A model using genetically engineered rats could be developed to observe the effects of dry eye over a longer period of time and mimic the chronicity seen in many human patients. Spontaneous development of dry eye due to specific endocrine imbalance has not been shown in any animal models to date. Nevertheless, orchiectomy and ovariectomy in rabbits, rats, mice, guinea pigs, and hamsters, and hypophysectomy in rats, have been used as models to study the influence of hormones on the structure and function of the lacrimal and meibomian glands (3). These procedures are not meant as an exact mimic of dry eye, but to decipher important pathogenic aspects of tear film regulation. Hormones have both direct and indirect effects on exocrine tissues due to their capacity to regulate immunity as well as the gene expression of many secreted molecules. For example, Sullivan, *et. al.* (2002), have demonstrated that androgens regulate the function of lacrimal glands and the quantity, quality, and metabolism of the lipid layer of the tear film produced by the meibomian glands (33). This may be an indication why women in the U.S. over the age of 50 display increased signs of dry eye because they have gone through menopause which causes a change in estrogen levels. Genetically modified mice are expected to aid in the study of the influence of a specific hormone(s) on the tear film homeostasis (3). Also, a naturally occurring model seen in rabbits or dogs could be a better model because many variables are eliminated, such as effect of scopolamine on the rest of the body, and would allow researchers to better gauge the natural progression of dry eye. Since scopolamine has no preference for one

of the different muscarinic subtypes, scopolamine will block the effects of acetylcholine at the muscarinic receptor throughout the body and brain and affect various physiological functions (43). It is not known what kind of effect or effects this would have during a dry eye study but it is a variable that needs to be taken into consideration when evaluating which model to use.

Another important aspect of the tear film that needs to be researched in further detail is the lipid layer. This is the outermost layer of the tear film and protects the aqueous layer from evaporating. It has been proven that artificial tears can offer relief to dry eye but not improve the underlying conditions that cause the disease. The key in discovering a cure for this disease could lie in how to control the lipid content of the tear film and how its secretion from the meibomian gland is controlled.

A novel aspect to this research study is the introduction of Restasis and FML to the model. It is important to see if these compounds that are used to treat the condition in humans have any effect on improving the symptoms of dry eye in animals so the model can be used to study new pharmacological treatments. Also, the OCT imaging and histological slices allow for us to look at cross sections of tissue *in vivo*. These images help to identify any changes in thinning of the cornea which has been revealed by Liu, *et. al.* (1999) to be an indicator of dry eye (46). Another benefit of the OCT imaging is that animals do not have to be sacrificed to look at cross sections of the cornea. This allows for better continuity in the study because data is being generated from the same animals across numerous time points.

Future studies would include molecular diagnostic methods. Harvesting tissue such as the cornea, conjunctiva, and lacrimal gland and then running mRNA analyses to compare protein production among tissues and groups would be a great addition to this model. The mRNA analysis could potentially identify biomarkers indicative of the

condition. For example, increased histamine levels in animals with dry eye could indicate an immune response and lead to a chemical cascade of other immunological agents. These protein levels of dry eye-induced animals and control animals could be compared side-by-side to help identify what's happening at a molecular level and categorize the severity of these reactions in regards to their contribution to dry eye symptoms. I would also add some histology procedures to the study. Hematoxylin and eosin staining would provide some basic front-line diagnostics and help identify any structural damage. Immunohistochemical techniques could help identify the locations of some of the biomarkers found in the mRNA analysis.

The scopolamine-induced dry eye model is a fairly new method of identifying clinical signs of dry eye. Research conducted by Viau, *et. al.* (2008) was the primary literature on which this study was based. Our model of dry eye does not include the molecular methods as used by Viau but they also did not use any means of measuring aqueous tear production (1). A 12.5 mg/day dose of scopolamine was used as recommended by Viau because it induced a moderate form of dry eye that is mainly seen in humans. A 25 mg/day dose was used in their study but induced a sever condition that is uncommon in humans. Another difference was Viau looked at a number of mucins and immuno-factors that are involved in the progression of dry eye but these hold no value in diagnosing the condition in a live patient.

The results from the fluorscein staining were mixed in comparison. Viau's dry eye animals averaged a score of 2.5 over three recorded time points whereas this study's scopolamine-induced dry eye animals averaged a score of around 3.5 over six time points. Viau's study is a great foundation for establishing a dry eye model but it has no clinical relevance. This study needs refining but there is more pure diagnostic value that can be used from tear volume measurements and *in vivo* cross sections of

the cornea.

Clinical Implications

This pre-clinical dry eye model is transferrable as a clinical dry eye model. If a patient schedules an appointment with their eye doctor and is complaining of symptoms analogous to dry eye, the doctor can run a battery of tests to help quickly and accurately diagnose the condition. First, they can place piece of phenol-red thread in each eye to determine tear volume. Next, they can place drops of fluorscein in each eye and record images of the corneal surface using cSLO. Then, they can look at a cross-section of the patient's eye using OCT to identify any thinning of the cornea without the need of a tissue sample. All of these procedures are non-invasive and can be performed in a matter of minutes at a clinic. If enough data is available, the doctor could compare the results of the tests to proven dry eye data and start the patient on treatment if necessary.

Synopsis

In summary, these experiments demonstrated continuous systemic administration of scopolamine to female Lewis rats and resulted in reduced tear volumes as measured during the 28 days following pump implantations. Thinning of the epithelium and stroma of the steroid-treated group indicates that dry eye was evident in Phase II, however, FML may not be as effective of a treatment as compared to saline drops or Restasis. Fluorescein corneal staining was increased, although high inter-animal variability prohibited definitive group comparisons. Furthermore, these experiments make a contribution to the field of dry eye study.

BIBLIOGRAPHY

1. Viau S, Maire MA, Pasquis B, Gregoire S, Fourgeux C, Acar N, Bretillon L, Creuzot-Garcher CP, Joffre C. Time course of ocular surface and lacrimal gland changes in a new scopolamine-induced dry eye model. *Graefes Arch Clin Exp Opthalmol*. 2008(246):857-67.

2. Viau S, Maire MA, Pasquis B, Gregoire S, Fourgeux C, Acar N, Bretillon L, Creuzot-Garcher CP, Joffre C. Efficacy of a 2-month dietary supplementation with polyunsaturated fatty acids in dry *eye induced by scopolamine in a rat model. Graefes Arch Clin Exp Opthalmol*. 2009(247):1039-50.

3. Barabino S, Dana MR. Animal models of dry eye: A critical assessment of opportunities and limitations. *Invest Ophthalmol Vis Sci*. 2004; 45(6):1641-6.

4. Fox SI. Human Physiology. Tenth ed. Boston: McGraw Hill; 2008.

5. Sherwood L, Klandorf H, Yancey PH. Animal Physiology: From genes to organisms. Australia: Brooks/Cole; 2005.

6. Smolek MK, Klyce SD. Duane's Foundations of Clinical Ophthalmology: Chapter 8 – The Cornea. Lippincott, Williams, and Wilkins; 2006.

7. Lu L, Reinach PS, Kao WWY. Corneal Epithelial Wound Healing. *Exp Biol Med*. 2001(226[7]): 653-664.

8. Epidemiology Subcommittee of the International Dry Eye Workshop. The epidemiology of dry eye disease: Report of the Epidemiology Subcommittee of the International Dry Eye Workshop. *Ocul Surf*. 2007(5[(2)]: 93–107.

9. Dartt DA. Duane's Foundations of Clinical Ophthalmology: Chapter 2 - The Conjunctiva: Structure and Function. Lippincott, Williams, and Wilkins; 2006.

10. Burkat CN, Hodges RR, Lucarelli MJ, Dartt DA. Duane's Foundations of Clinical Ophthalmology: Chapter 2A - Physiology of the Lacrimal System. Lippincott, Williams, and Wilkins; 2006.

11. Gipson IK. The Ocular Surface: The Challenge to Enable and Protect Vision *Invest Ophthalmol Vis Sci*. 2007(48[10]); 4391-4398.

12. Peters E, Colby K. Duane's Foundations of Clinical Ophthalmology: Chapter 3 - The Tear Film. Lippincott, Williams, and Wilkins; 2006.

13. Takahashi M, Ishimaru N, Yanagi K, Haneji N, Saito I, Hayashi Y. High Incidence of autoimmune dacryoadenitis in male non-obese diabetic (NOD) mice depending on sex steroid. *Clin Exp Immunol.* 1997; 109:555-561.

14. Humphreys-Beher MG, Hu Y, Nakagawa Y, Wang PL, Purushotham KR. Utilization of the non-obese diabetic (NOD) mouse as an animal model for the study of secondary Sjögren's syndrome. *Adv Exp Med Biol.* 1994; 350:631-636.

15. Van Blokland SC, Versnel MA. Pathogenesis of Sjögren's syndrome: characteristics of different mouse models fro autoimmune exocrinopathy. *Clin Immunol.* 2002; 103:111-124.

16. Toda I, Sullivan BD, Rocha EM, Da Silveria LA, Wickham LA, Sullivan DA. Impact of gender on exocrine inflammation in mouse models of Sjögren's syndrome. *Exp Eye Res.* 1999; 69:355-366.

17. Jabs DA, Lee B, Whittum-Hudson J, Prendergast RA. The role of Fas-Fas ligand-mediated apoptosis in autoimmune lacrimal gland disease in MRL/MpJ mice. *Invest Ophthalmol Vis Sci.* 2001; 42:399-401.

18. Jabs DA, Lee B, Whittum-Hudson J, Prendergast RA. Th1 versus Th2 immune responses in autoimmune lacrimal gland disease in MRL/Mp mice. *Invest Ophthalmol Vis Sci.* 2000; 41:826-831.

19. Gilbard JP, Hanninen LA, Rothman RC, Kenyon KR. Lacrimal gland, cornea, and tear film in the NZB/NZW F_1 hybrid mouse. *Curr Eye Res.* 1987; 6:1237-1248.

20. McCartney-Francis NL, Mizel DE, Frazier-Jessen M, Kulkarni AB, McCarthy JB, Wahl SM. Lacrimal gland inflammation is responsible for ocular pathology in TGF-β1 null mice. *Am J Pathol.* 1997; 141:1281-1288.

21. McCartney-Francis NL, Mizel DE, Redman RS, et al. Autoimmune Sjögren's-like lesions in salivary glands in TGF-β1-deficient mice are inhibited by adhesion blocking peptides. *J Immunol.* 1996; 157:1306-1312.

22. Tsubata R, Tsubata T, Hiai H, et al. Autoimmune disease of exocrine organs in immunodeficient alymphoplasia mice: a spontaneous model for Sjögren's syndrome. *Eur J Immunol.* 1996; 26:2742-2748.

23. Konno A, Takada K, Saegusa J, Takiguchi M. Presence of B7-2^+ dendritic cells and expression of Th1 cytokines in the early development of sialodacryoadenitis in the IQI/Jic mouse model of primary Sjögren's syndrome. *Autoimmunity.* 2003; 36:247-254.

24. Hayashi Y, Haneji N, Hamano H, Yanagi K. Transfer of Sjögren's syndrome-like autoimmune lesions into SCID mice and prevention of lesions by anti-CD4 and anti-T cell receptor antibody treatment. *Eur J Immunol*. 1994; 24:2826-2831.

25. Wharen M, Solomin L, Pettersson I, Isenberg D. Autoantibodies repertoire to Ro/Ssa and La/SSB antigen in patients with primary and secondary Sjögren's syndrome. *J Autoimmun*. 1996; 9:537-544.

26. Ulbricht K, Schmidt RE, Witte T. Antibodies against α-fodrin in Sjögren's syndrome. *Autoimmun Rev*. 2003; 2:109-113.

27. Bacman S, Berra A, Sterin-Borda L, Borda E. Muscarinic acetylcholine receptor antibodies as a new marker of dry eye Sjögren syndrome. *Invest Ophthalmol Vis Sci*. 2001; 42:321-327.

28. Robinson CP, Brayer J, Yamachika S, et al. Transfer of human serum IgG to nonobese diabetic $Ig\mu^{null}$ mice reveals a role for autoantibodies in the loss of secretory function of exocrine tissues in Sjögren's syndrome. *Proc Natl Acad Sci USA*. 1998; 95:7538-7543.

29. Nguyen KH, Brayer J, Cha S, et al. Evidence for antimuscarinic acetylcholine receptor antibody-mediated secretory dysfunction in NOD mice. *Arthritis Rheum*. 2000; 43:2297-2306.

30. Zhu Z, Stevenson D, Schechter JE, Mircheff AK, Atkinson R, Trousdale MD. Lacrimal histopathology and ocular surface disease in a rabbit model of autoimmune dacryoadenitis. *Cornea*. 2003; 22:25-32.

31. Liu SH, Prendergast RA, Silverstein AM. Experimental autoimmune dacryoadenitis. I. Lacrimal gland disease in the rat. *Invest Ophthalmol Vis Sci*. 1987; 28:270-275.

32. Maitchouk DY, Beuerman RW, Ohta T, Stern M, Varnell RJ. Tear production after unilateral removal of the main lacrimal gland in squirrel monkeys. *Arch Ophthalmol*. 2000; 118:246-252.

33. Sullivan DA, Sullivan BD, Evans JE, et al. Androgen deficiency, meibomian gland dystfunction, and evaporative dry eye. *Ann NY Acad Sci*. 2002; 966:211-222.

34. Stern ME, Beuerman RW, Fox RI, Gao J, Mircheff AK, Pflugfelder SC. The pathology of dry eye: the interaction between the ocular surface and lacrimal glands. *Cornea*. 1998; 17:584-589.

35. Burgalassi S, Panichi L, Chetoni P, Saettone MF, Boldrini E. Development of a simple dry eye model in the albino rabbit and evaluation of some tear substitutes. *Ophthalmic Res*. 1999; 31:229-235.

36. Zoukhri D, Hodges RR, Dartt DA. Ca^{2+} signaling by cholinergic and α_1-adrenergic agonists is up-regulated in lacrimal and submandibular glands in a murine model of Sjögren's syndrome. *Clin Immunol Immunopathol*. 1998; 89:134-140.

37. Fujihara T, Nagano T, Nakamura M, Shirasawa E. Establishment of a rabbit short-term dry eye model. *J Ocul Pharmacol Ther*. 1995; 11:503-508.

38. Gilbard JP, Rossi SR, Heyda KG. Tear film and ocular surface changes after closure of the meibomian gland orifices in the rabbit. *Ophthalmology*. 1989; 96:1180-1186.

39. Rolando M, Refojo MF. Tear evaporimeter for measuring water evaporation rate from the tear film under controlled conditions in humans. *Exp Eye Res*. 1983; 36:25-33.

40. Dursun D, Wang M, Monroy D. et al. A mouse model of keratoconjunctivitis sicca. *Invest Ophthalmol Vis Sci*. 2002; 43:632-638.

41. Gao J, Shwalb TA, Addeo JV, Ghosen CR, Stern ME. The role of apoptosis in the pathogenesis of canine keratoconjunctivitis sicca: the effect of topical cyclosporin A therapy. *Cornea*. 1998;17:654-663.

42. Kaswan R, Pappas C Jr, Wall K, Hirsch SG. Survey of canine tear deficiency in veterinary practice. *AdvExp Med Biol*. 1998; 438:931-939.

43. Blokland A. Scopolamine-induced deficits in cognitive performance: A review of animal studies. Faculty of Psychology, Brain & Behavior Institute, Maastricht University, The Netherlands; 2005.

44. ALZET Osmotic Pump Specifications Manual. DURECT Corporation; 2012.

45. Wecker L, Crespo LM, Dunaway G, Faingold C, Watts S. Brody's Human Pharmacology: Molecular to Clinical. Mosby; 2010.

46. Liu Z, Pflugfelder SC. Corneal thickness is reduced in dry eye. *Cornea*. 1999(18[4]):403-407.